scientific reports

Check for updates

OPEN

BRSK2 plays a role in autophagy and cancer cell growth and survival under nutrient deprivation stress via the PIK3C3 pathway

Aparna Maiti[1,2]✉, Alison D. Axtman[3], Rongrong Wu[1], Lydia J. B. Redman[1], Kazuaki Takabe[1], Aimee B. Stablewski[2,4], Li Yan[5], Michael J. Ciesielski[6,7], Jianmin Zhang[8], Sharon S. Evans[9], Pawel Kalinski[9,10] & Nitai C. Hait[1,2]✉

Macroautophagy/autophagy is a stress-responsive lysosomal catabolic pathway that promotes cellular homeostasis and tumor cell survival, but its role in breast cancer progression and metastasis remains unclear. Here, we show that a brain-specific serine/threonine protein kinase, BRSK2, a marker of aggressive metastatic disease in breast cancer patients, is crucial in regulating autophagy. BRSK2 is overexpressed in aggressive cancer and is associated with reduced disease-specific survival. BRSK2 also regulates basal autophagy and activates AKT, STAT3, and NF-κB-mediated cancer cell survival pathways. In addition, BRSK2 overexpression increases the levels of inflammatory cytokines and chemokines in breast cancer cells. Downregulation of BRSK2 using specific siRNAs or the BRSK2 kinase small-molecule inhibitor GW296115 markedly reduced nutrient-deprivation stress-mediated autophagy, cell growth, and metastatic potential, and enhanced breast cancer cell apoptosis. Endogenous BRSK2 is associated with the Vps34-class III PI3K-Beclin-1-ATG14 autophagy signaling complexes that could protect cancer cells from nutrient-deprivation stress. Our findings demonstrate the key role of the BRSK2-mediated protective autophagy and cell growth and survival under nutrient deprivation stress via survival signals, e.g., PI3K/AKT or STAT3-NF-kB, in aggressive breast cancer cells.

Keywords BRSK2, Breast cancer, Autophagy, Nutrient-deprivation stress, Cell survival

Abbreviations

BRSK	Brain-specific serine/threonine protein kinase
LC3	Microtubule-associated protein 1 light chain 3 alpha
AMPK	5′ Adenosine monophosphate-activated protein kinase
LKB1	Liver kinase B1
PI3K	Phosphoinositide 3-kinase
PKB	Protein kinase B
STAT3	Signal transducer and activator of transcription 3
NF-κB	Nuclear factor kappa B
Vps34	Vacuolar protein sorting 34
ER	Estrogen receptor

[1]Division of Breast Surgery and Department of Surgical Oncology, Roswell Park Comprehensive Cancer Center, Buffalo, NY, USA. [2]Department of Molecular & Cellular Biology, Roswell Park Comprehensive Cancer Center, Elm & Carlton Streets, Buffalo, NY 14263, USA. [3]Structural Genomics Consortium, UNC Eshelman School of Pharmacy, University of North Carolina at Chapel Hill, Chapel Hill, NC 27599, USA. [4]Roswell Park Comprehensive Cancer Center, Gene Targeting and Transgenic Shared Resource, Buffalo, NY, USA. [5]Department of Biostatistics & Bioinformatics, Roswell Park Comprehensive Cancer Center, , Buffalo, NY 14263, USA. [6]Department of Neurosurgery, Roswell Park Comprehensive Cancer Center, Buffalo, NY, USA. [7]MimiVax LLC, Buffalo, NY, USA. [8]Department of Cell and Cancer Biology, The University of Toledo College of Medicine and Life Sciences, Toledo, OH 43614, USA. [9]Department of Immunology, Roswell Park Comprehensive Cancer Center, Buffalo, NY 14263, USA. [10]Department of Medicine, Roswell Park Comprehensive Cancer Center, Buffalo, NY 14263, USA. ✉email: Aparna.Maiti@Roswellpark.org; Nitai.Hait@Roswellpark.org

TNBC	Triple-negative breast cancer
TCGA	The Cancer Genome Atlas
METABRIC	Molecular Taxonomy of Breast Cancer International Consortium
DSS	Disease-specific survival
PFI	Progression-free interval
PFS	Progression-free survival
OS	Overall survival
EMT	Epithelial-mesenchymal transition
SCLC	Small cell lung cancer
PDAC	Pancreatic ductal adenocarcinoma
TEM	Transmission electron microscopy
siRNA	Small interfering RNA
CRISPR	Clustered regularly interspaced short palindromic repeats
RT	Room temperature
OE	Overexpression
KD	Knockdown
WT	Wild-type
CT	Cycle threshold
qPCR	Quantitative polymerase chain reaction
SDS-PAGE	Sodium dodecyl-sulfate polyacrylamide gel electrophoresis
HEK	Human embryonic kidney

Although tumor metastasis is the foremost cause of cancer-related death among breast cancer patients, druggable functional biomarker proteins and effective therapeutic strategies targeting the prevention of metastasis remain limited[1]. Furthermore, tumor cell metastasis is a multi-step process; at each step, the tumor cell must survive in a stressful environment, such as hypoxia, energy deprivation, or nutrient deprivation. Macroautophagy/autophagy is an evolutionarily conserved catabolic mechanism that is induced in response to various stresses and plays a critical role in each step of the metastatic cascade[2–5]. However, the mechanism by which autophagy regulates tumor metastasis remains unknown. Nevertheless, the autophagy process has been reported to have both pro- and anticancer properties, as uncontrolled autophagy induced by severe stress or many anticancer drugs can enhance autophagy and autophagic cell death[3]. Several recent publications have implicated autophagy associated with drug-resistant tumor cell survival, epithelial-mesenchymal transition (EMT) in tumor metastasis[6], and inflammation[7,8]. Autophagy has a cytoprotective role in anoikis resistance[9,10] and promotes the survival of dormant tumor cells[11], resulting in metastatic growth. In addition, high expression of microtubule-associated protein 1A/1B-light chain 3B (LC3B), a central protein in autophagy in solid tumors, is associated with higher proliferative tumor cells, tumor metastasis, and poor outcome in cancer patients[12], reinforcing that autophagy is a promising mechanism in tumor metastasis. However, induction of autophagy also results in the suppression of tumor progression and migration by various mechanisms, indicating that autophagy also has metastasis-preventing functions[13,14]. So far, targeting the autophagy mechanism associated with tumor cell survival is partially successful in the clinical setting[15,16]; thus, a molecular understanding of the regulatory mechanisms of autophagy in cancer is essential.

Physiologically, autophagy is an essential homeostatic mechanism whereby dysfunctional protein aggregates or organelle components are engulfed in a double-membrane vesicle called an autophagosome and delivered to lysosomes for degradation and recycling to crucial cellular components[17–19]. Some tumor cells exhibit higher basal autophagy levels for their oncogenic events, even under normal conditions. Further, tumor cells depend more on autophagy than normal cells for an alternate energy source to cope with their metabolic demands[20]. The active unc-51 generally induces cellular canonical autophagy, such as the autophagy autophagy-activating kinase 1 (ULK1) protein complex; otherwise, autophagy signaling is blocked by the mechanistic target of rapamycin kinase (mTOR) complex 1 (mTORC1). Autophagy is mainly regulated by 5′ adenosine monophosphate-activated protein kinase (AMPK) downstream of the liver kinase LKB1, involving several cellular mechanisms in response to metabolic stress and maintaining energy homeostasis[21]. AMPK activation, together with mTORC1 inactivation in response to nutrient deprivation stress, directly phosphorylates the autophagy initiator protein kinase ULK1, thereby activating downstream components of the phosphoinositide 3-kinase class III Vps34 (also known as PIK3C3) complexes and recruiting the ATG14 complex, including Beclin-1, for LC3 lipidation (LC-II) and subsequent double-membrane structured autophagosome formation, a key event for the process of autophagy[22,23]. The AMPK signaling pathway coordinates cell-intrinsic autophagy and metabolism under low-energy conditions[24].

Nothing is known about the brain-specific serine/threonine protein kinases BRSK2 and BRSK1, the AMPK-related kinases, in regulating autophagy, particularly the mechanisms involved in autophagy-mediated tumor cell survival or autophagic cell death in response to nutrient-deprived stress. BRSK2 and BRSK1, also known as synapses of amphids defective (SAD) kinase SAD-A and SAD-B, respectively, downstream of the LKB1, are one of the dark/underinvestigated kinases recently defined by the National Institutes of Health (NIH) Illuminating the Druggable Genome (IDG) program; their functions are uncharacterized in cancer. BRSK2 and BRSK1 kinases are known to be activated by LKB1, PAK1, CAMKII, and PKA[25–27]. BRSK2 and BRSK1 kinases are mainly expressed in the human brain[28] and result in neuronal polarization and brain development[29]. Furthermore, the loss of these kinases results in early neuronal apoptosis and a reduced number of progenitors, suggesting these kinases are required to survive cortical neurons[30]. Besides the brain, these kinases were also expressed at lower levels in the testis and pancreas[25]. BRSK2 promotes insulin secretion in response to glucose stimulation in pancreatic islets[27,31,32].

To date, similar to AMPK, BRSK2 kinase is induced by starvation to inhibit mTOR via phosphorylating the Tuberous Sclerosis Complex (TSC)-2, promote autophagy, and recent studies suggested that BRSK2 activation leads to activation of PI3K/AKT signaling[31,33–38]. Published results indicated that PI3K/AKT can be involved in both upstream and downstream regulation of mTORC1[39]. Activation of mTORC1 strongly represses upstream PI3K/AKT signaling by the potent negative feedback loop and functions as a brake for AKT[40]. Therefore, new studies suggested that the repression of mTOR by starvation-induced BRSK2 may cause a loss of feedback inhibition on AKT activation[34].

However, the biological significance of BRSK2 kinase's direct involvement in autophagy and cell fate in tumor cells in response to nutrient deprivation stress is unknown. Here, we identify the clinical relevance of BRSK2 expression in breast cancer patients. Furthermore, we have determined how specifically BRSK2 kinase directly regulates autophagy and is involved in tumor cell growth and survival in response to nutrient-deprived stress.

Results

Elevated BRSK2 expression correlates with poor prognosis and disease recurrence in breast cancer patients

To investigate the clinical relevance of the understudied serine/threonine kinase, BRSK2, in breast cancer, we have analyzed publicly available RNA-Seq datasets—i.e., The Cancer Genome Atlas (TCGA)[41] and Molecular Taxonomy of Breast Cancer International Consortium (METABRIC)[42] cohorts—which include the gene expression profiles and clinical information of patients. BRSK2 protein has been reported as overexpressed in PDAC patients and is involved in PDAC cell survival[34,43]. First, our analyses depicted that the breast tissue expression levels of *BRSK2* were significantly higher in the groups with cancer and relapsed or recurrent disease compared to the adjacent non-malignant normal tissue of patients (Fig. 1A, B). Importantly, *BRSK2* expression in breast cancer patients appears to be correlated with the aggressive stage of breast cancer and marginally elevated in TNBC aggressive subtypes compared with ER + breast cancer patients Fig. 1C, D). We have also analyzed the survival rates of breast cancer patients (top vs. bottom thirds of patients as per normalized tumor gene expression) using the Kaplan–Meier method with a log-rank test. Disease-specific survival (DSS) and progression-free interval (PFI) or progression-free survival (PFS) in the TCGA breast cancer cohort (hazard ratio [HR] = 2.739, lower 95% confidence interval (CI) of HR = 1.643, upper 95% CI of HR = 4.566, $p = 0.0002$; HR = 1.489, lower 95% CI of HR = 1.005, upper 95% CI of HR = 2.205, $p < 0.05$, respectively) and overall survival (OS) in METABRIC cohort (HR = 1.172, lower 95% CI of HR = 1.014, upper 95% CI of HR = 1.355, $p < 0.05$) was significantly lower, which indicates that *BRSK2* overexpression confers a high risk of progressive disease in patients (Fig. 1E, Fig. S1A). Next, we further analyze *BRSK2* mRNA expression in primary tumor tissues to examine whether it correlates with clinical outcomes (e.g., metastasis) in patients with breast cancer. Using qPCR analysis, we observed that *BRSK2* was significantly elevated in every patient's primary breast tissue who had a history of metastasis (n = 10) compared to those patients (n = 10) who had never metastasized to any organs for 10 years (Fig. 1F)[44].

Previously, BRSK1, another related serine/threonine kinase of BRSK2, although it shares similar biological functions with the BRSK2[29], has been implicated as a tumor suppressor, LKB1 downstream gene, decreased in breast cancer[45], and a putative mutated loss-of-function gene in gastric and colorectal cancers[46]. Although *BRSK1* transcript levels appeared elevated in our data analysis in the groups with cancer and metastatic disease compared to adjacent non-malignant normal tissue of patients, *BRSK1* transcript levels, however, do not appear to be correlated with the aggressive disease clinical parameters or patients' survival rate (Fig. S1B–F).

These data suggest that the *BRSK2* transcript levels may be an essential predictive risk factor for metastatic diseases in breast cancer patients.

The BRSK2 expression level is increased in breast cancer cells

To gain further insights into BRSK2 expression in breast cancer cell models, we first assessed an array of human breast cancer cell lines (estrogen receptor [ER]-positive and triple-negative breast cancer [TNBC]) vs. control mammary epithelial MCF10A to analyze BRSK2 protein and BRSK2 mRNA expression. Our data revealed that BRSK2 protein and *BRSK2* transcripts are elevated in most human breast tumor cells compared to normal mammary epithelial MCF10A cells (Fig. 2A, B). Data further uncovered that BRSK2 is overexpressed amongst various breast cancer subtype-specific human cell lines, including luminal and TNBC cells. MCF10A has almost no expression of BRSK2 (Fig. 2A). BRSK2 is overexpressed amongst different ER-positive human breast cancer cell lines, including MCF-7, T-47D, ZR-75-1, and BT-474. Among human TNBC cell lines, we observed higher BRSK2 protein expression in BT-549 (14-fold) than in SUM-149 (1.4-fold)(Fig. 2A). We used different metastatic variants of parental TNBC MDA-MB-231 to examine the expression level of BRSK2. Interestingly, we found that the TNBC lung metastatic variant LM-2–4 (8.5-fold) and brain-metastatic variant MDA-MB-231BR cells (11-fold) have increased expression compared to the parental MDA-MB-231 cells (sixfold), suggesting BRSK2 signaling may be involved in tumor metastasis (Fig. 2A). As the BRSK2 protein has an unequal expression in the human breast cancer cell SUM-149 compared with the rest of the cancer cell lines, we became interested in examining the transcript level of *BRSK2*. We found that MCF10A has almost no transcript expression, supporting protein expression data, confirming that normal epithelial breast cells do not express *BRSK2*. Interestingly, protein expression data reciprocally match transcript data in all breast cancer cell lines except SUM-149 cells (Fig. 2B). For instance, MCF-7 and LM2-4 cells have high protein (sixfold and 8.5-fold, respectively) and mRNA expression (sevenfold and tenfold, respectively), lung-metastatic LM-2 and brain-metastatic MDA-MB-231BR have higher mRNA expression (tenfold and 11-fold, respectively) and higher protein expression (8.5-fold and 11-fold, respectively) compared with the parental TNBC MDA-MB-231 cells (protein expression, sixfold and mRNA expression eightfold). Based on our data, the *BRSK2* transcript and protein were elevated in breast tumor cells or metastatic breast cancer cells compared with nonmalignant epithelial cells. The complex regulation

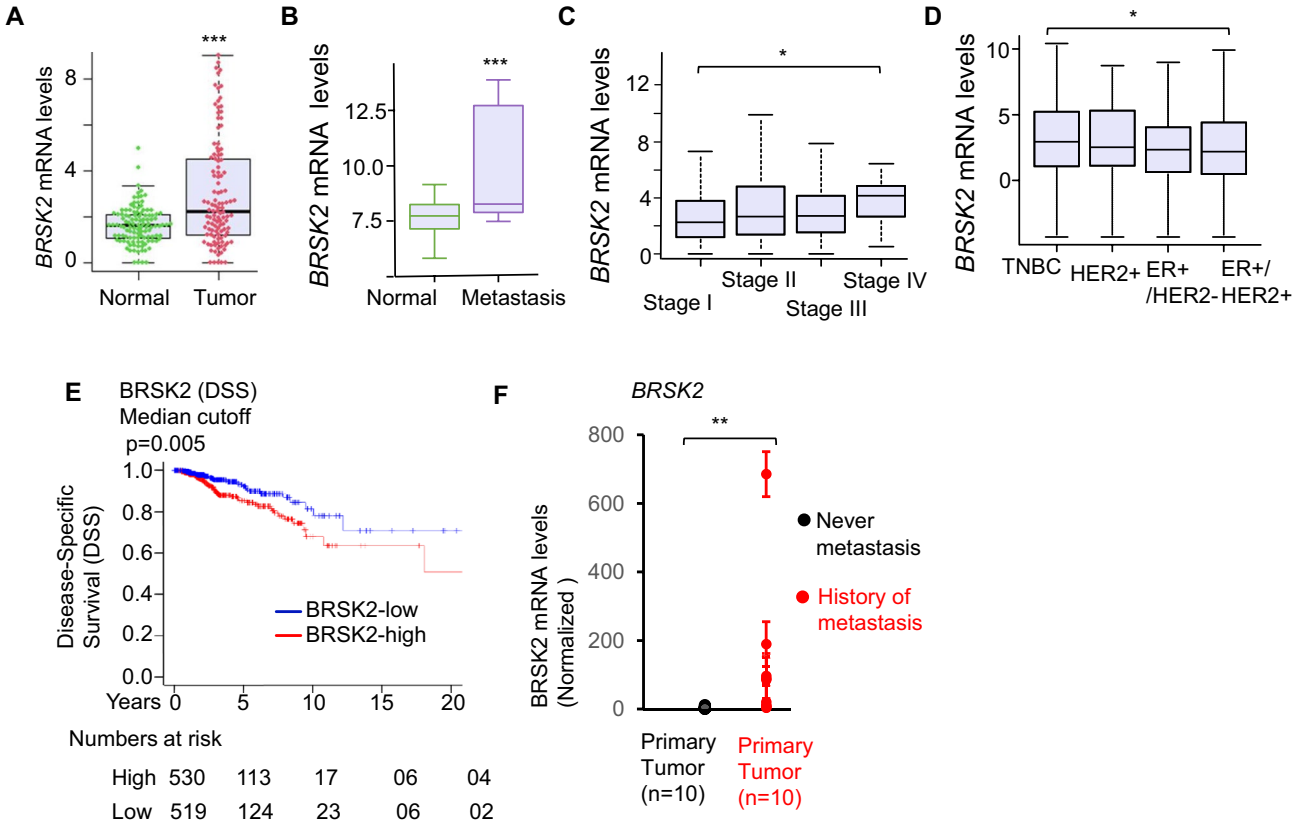

Fig. 1. BRSK2 expression correlates with clinical outcomes in patients with breast cancer. (**A**) Boxplots show elevated log2 expression of BRSK2 mRNA in breast cancer patients from the TCGA-BRCA whole cohort (n = 1092) compared to normal adjacent breast tissue (n = 112). ***$p < 0.001$ (tumor vs. normal). (**B**) Boxplots show elevated *BRSK2* transcript levels in metastatic patients (n = 7) from the TCGA-BRCA cohort compared to normal adjacent breast tissues (n = 112). (**C**) Boxplots of high expression of *BRSK2* mRNA of tumors of different American Joint Committee on Cancer (AJCC) stages for TCGA-BRCA cohort. (**D**) Boxplots of high BRSK2 expression score by immunohistochemistry (IHC) determined subtype in the TCGA-BRCA cohort. All boxes are presented as medians with interquartile range. Mann–Whitney U and Kruskal–Wallis H tests were used for the analysis. For some figures, significant *p*-values are shown. *$p < 0.05$ was considered significant. (**E**) Kaplan–Meier plots with log-rank *p*-values for disease-specific survival (DSS) in the TCGA-BRCA cohort, stratified by *BRSK2* mRNA expression. Adverse DSS with higher BRSK2 transcripts was found in the TCGA-BRCA cohort, and the log – rank test was used for the analysis. The median split patients and significant *p*-values are shown ($p = 0.005$). (**F**) *BRSK2* transcripts were analyzed by quantitative PCR (qPCR) in patients with primary tumors. Primary tumors (never-metastatic, n = 10) and age-matched primary tumors from patients with a history of metastasis (n = 10)[44] were used for qPCR analysis of *BRSK2* and *GAPGH* as a housekeeping control gene. Normalized *BRSK2* gene levels to *GAPDH* ($2^{\wedge -delta}$ CTx10,000) are shown. The student's t-test, **$p < 0.01$, is significant in experimental triplicate.

between protein and mRNA exists in SUM-149 (Fig. 2A, B). Earlier studies have suggested that BRSK2's regulatory mechanism promotes its degradation in the ubiquitin–proteasome pathway, which may partly explain the discordance between BRSK2 protein and *BRSK2* transcript levels[47,48]. We have excluded SUM-149 for further analysis of BRSK2 expression since highly tumorigenic SUM-149 IBC cells are pathologically distinct from the rest of the non-IBC TNBC cells examined, and SUM-149 is mainly used for the study of inflammatory breast cancer[49]. In contrast to BRSK2 overexpression in most human breast cancer cells, BRSK1 expression is silenced[45,46] in all the human breast cancer cells examined (Fig. S2A, B).

BRSK2 is overexpressed in cancer compared with normal breast tissue or normal breast nonmalignant epithelial cells and is associated with progressive disease phenotypes.

BRSK2 activates AKT and STAT3- and NF-κB-mediated cancer cell survival signaling pathways

Phosphatidylinositol 3-kinase (PI3K)-AKT, master transcription factors STAT3, and NF-κB signaling are among the most critical intracellular pathways, which can be considered master regulators for cancer cell survival[50–56]. To examine the role of BRSK2 expression on cancer cell survival pathways, we transiently overexpressed BRSK2 in breast cancer cells compared to an empty vector control and subjected them to western blotting using 1D and 3D cell culture models. *The* in vitro 3D cell culture model is representative of the in vivo tumor environment,

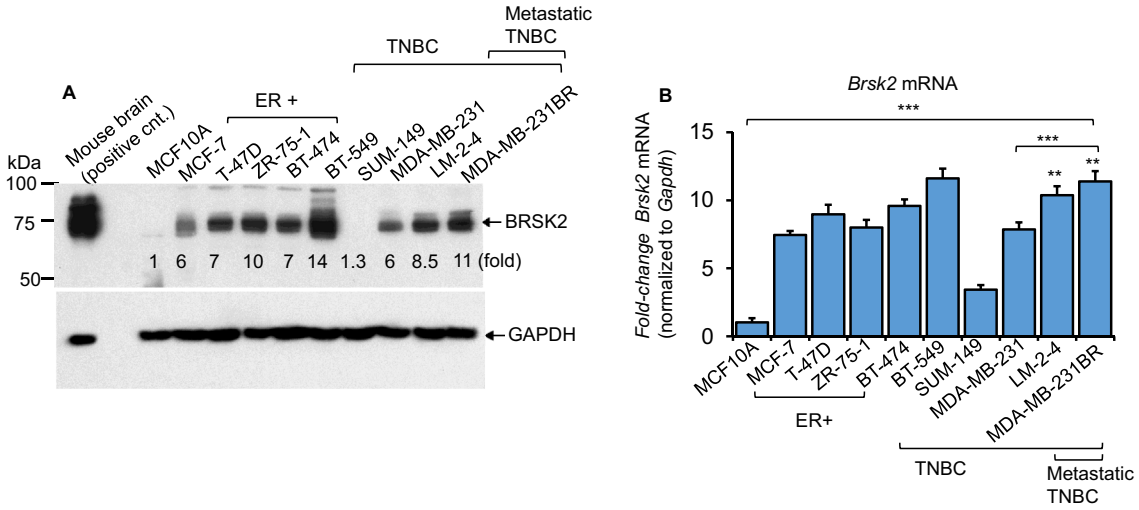

Fig. 2. BRSK2 is elevated in human breast cancer cells vs. benign tumor cells. (**A**), Total cell lysates from normal human breast epithelial cell lines (MCF10A), an array of human breast cancer ER+ cell lines, and TNBC and metastatic TNBC cell lines were used for western blot analysis with the antibodies against BRSK2 (**A**). Since BRSK2 is primarily expressed in the brain, a mouse whole-brain protein extract was used as a positive control for BRSK2 protein expression. GAPDH was used to show equal loading and transfer. N = 3, representative blots were shown. The BRSK2 protein band (78–90 kDa) in the western blot. (**B**) Total RNA was isolated separately from individual cells and treated with DNase. cDNA was prepared from total RNA and used for SYBR-Green qPCR analysis for *BRSK2* transcript expression. *GAPDH* mRNA expression was used to normalize *BRSK2* transcript levels. Normalized transcript expression levels were calculated using the Delta CT method (n = 3); data are means ± s.e. One-way ANOVA (***$p < 0.001$), Student's t-test, and ***$p < 0.001$ (metastatic TNBC cell vs. parental TNBC cell). *Note*: Normalized *BRSK2* mRNA levels are significantly elevated (***$p < 0.001$, cancer cells vs. MCF10A).

featuring a hypoxic, nutrient-deficient core that undergoes epigenetic changes and is enriched with cancer stem cells (CSCs)[57–59]. Overexpression of BRSK2 vs. empty vector control markedly enhances AKT activity and NF-κB activity (phospho-NF-κB, S536) in the 1D culture of BT-474 (Fig. 3A), MDA-MB-231 (Fig. 3B), and MDA-MB-231BR (Fig. 3C) cells, which is a metastatic variant of MDA-MB-231 cells. Interestingly, our 3D MDA-MB-231BR cell model data, as shown in Fig. 3D, suggest that overexpression of BRSK2 compared to the empty vector profoundly elevates active AKT (S473), STAT3 (Y705 and S727), and NF-κB (S536) cell signaling molecules. Cytokines or growth factors signaling activate the master transcription factors STAT3 and NF-κB[60]. These activated dimerized transcription factors translocate to the nucleus and transcribe specific genes important for cancer cell growth and survival[61,62]. Our western blotting data after isolating pure nuclear and nuclei-free cytosolic fractions (Fig. 3E, F) showed that overexpression of BRSK2 vs. empty vector in BT-474 (Fig. 3E) and MDA-MB-231 (Fig. 3F) cells markedly enhanced translocation of STAT3 (Y705) and p65-NF-κB into the nucleus or BRSK2 vs. empty vector stably transfected in MDA-MB-231 cells (Fig. S3) enhanced translocation of p65-NF-κB into the nucleus, reconfirming the activation of these transcription factors by BRSK2. Next, we have confirmed that some of the known STAT3 or NF-κB-mediated inflammatory cytokines, such as IL-6, TNF-α, IL-1β, CXCL1, and CXCL6, are strongly regulated by BRSK2 in breast cancer cells (Fig. S4). Although BRSK1 has been implicated as a tumor suppressor, our data indicate that BRSK1 is silenced in breast cancer cells. Ectopic expression of BRSK1, similar to BRSK2, enhances AKT, STAT3, and NF-κB-mediated cancer cell survival signaling pathways in breast cancer cells. Our data suggested that BRSK2 plays a vital role in regulating PI3K-AKT, STAT3, and NF-κB-mediated cell growth and survival pathways.

BRSK2 expression promotes nutrient-deprived stress-mediated autophagy in breast cancer cells

Nutrient-deprived and hypoxic microenvironments are the common characteristics of breast tumors due to insufficient blood supply. Extended lengths of nutrient deprivation stress can influence the metastatic potential of tumor cells[63,64]. AMPK-related groups of protein kinases are suggested to have a role in controlling autophagy in response to nutrient starvation[33]. Since BRSK2 is one of the AMPK-related protein kinases expressed at a higher level in breast cancer[26,35,36], we have examined whether BRSK2 expression regulates autophagy in response to various energetic stresses (glucose, glutamine, or nutrient deprivation) in breast cancer cells. In cellular modeling, we ectopically overexpressed BRSK2 in hormone receptor (HR) positive and triple-negative breast cancer (TNBC) human cell lines. Using BT-474, one of the moderate BRSK2-expressing cell lines, we transiently overexpressed BRSK2 and an empty vector, followed by exposure to glucose alone or glucose and glutamine, or nutrient-null conditions for increasing time points up to 6 h. Immunoblotting analysis showed that LC3-II protein (a lipid-conjugated form of LC3, a key marker of autophagosome formation), an indicator of autophagy[23], was increased in BRSK2 overexpression vs. empty vector in response to glucose alone, glucose

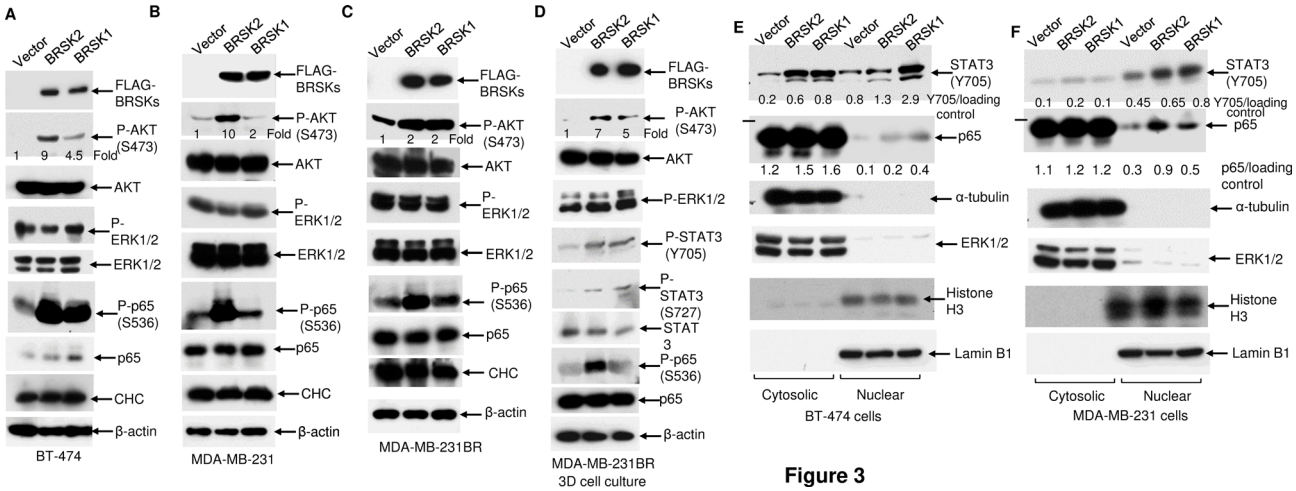

Figure 3

Fig. 3. BRSK2 ectopic expression in breast cancer cells is associated with tumor cell survival pathways linked to AKT and activation of master transcription factors STAT3 and NF-κB. BT-474 (**A**), MDA-MB-231 (**B**), and MDA-MB-231/BR (**C**) cells were transfected with the empty vector, BRSK2, or the BRSK1 plasmids for 48 h, and total protein lysates were prepared for western blot analysis with the indicated antibodies. For some experiments, 3D cell cultures were established 24 h after plasmid transfection. (**D**) MDA-MB-231/BR cells, as shown, were grown for an additional 48 h in a low-attachment six-well plate to form tumorospheres (see Materials and Methods). Total protein lysates were prepared for western blot analysis, as indicated, including phospho-AKT (Ser473), phosphor-STAT3 (Ser727 and Tyr705), and phospho-NF-κB (Ser536) antibodies. CHC and β-actin antibodies were used for equal loading and transfer. Anti-FLAG antibodies were used for FLAG-tagged BRSK2 protein expression. n = 3, representative blots are shown. Duplicate BT-474 (**A**) and MDA-MB-231 (**B**) cell cultures were used to isolate nuclear and cytosolic fractions, free of nuclei, using established protocols. (**E** and **F**) As indicated, equal amounts of nuclear and cytosolic proteins were used for Western blotting, using specific antibodies against the target proteins. Translocation of p65-NF-κB or active STAT3(Y705) into the nucleus in response to ectopic BRSK2 or BRSK1 expression vs. empty vector was observed in both BT474 (**E**) and MDA-MB-231 (**F**) cell models. α-tubulin and total ERK1/2 antibodies, as well as histone H3 and Lamin B1 antibodies, were used to identify cytosolic and nuclear protein markers, respectively, free of nuclei. n = 3, representative blots were shown. Scanned blots and fold intensities normalized to respective loading control vs. vector control were labeled (ImageJ).

and glutamine, or nutrient starvation for 6 h, indicating that BRSK2 expression regulates autophagy[65,66] in BT-474 cells (Fig. 4A). To confirm the role of BRSK2 in the nutrient-deprived-stress-induced accumulation of autophagosomes in breast cancer cells, we further measured LC3-II protein levels (β-actin as a loading control-normalized LC3-II levels), rather than the normalized LC3-II/LC3-I ratio, which correctly reflects changes in autophagy[67–71] in BRSK2 overexpressing vs. vector-transfected BT-474 cells. Our data showed that BRSK2 overexpression significantly enhances autophagy in these cells in response to nutrient starvation at both 2-h and 6-h time points. We observed that the basal level of LC3-II is higher in breast cancer cells, and nutrient-deprivation stress marginally enhanced autophagy in these cells (Fig. 4B). Overexpression of BRSK2 also enhanced the expression of other autophagy-related proteins, including Beclin-1, ATG3, and ATG5 (Fig. 4A). Consistent with the concept that BRSK2 expression protects cells from nutrient stress via AKT activation[34], we also found that BRSK2-overexpressing cells exhibit persistent activation of AKT at the later time point of nutrient starvation (6 h) compared to vector-transfected cells (Fig. S5A). P-ERK1/2 levels tend to be enhanced in the BRSK2 overexpressed cells vs. vector-transfected cells in response to glucose starvation or nutrient starvation at the later time point (6 h)(Fig. S5A). Consistent with BT-474 cells, BRSK2 overexpression enhanced LC3-II and Beclin-1 protein levels to similar stress conditions as in (Fig. 4A, B) in TNBC brain-metastatic MDA-MB-231BR cells (Fig. S5B).

Next, we further monitored GFP-LC3 autophagic puncta formation[65,67] using GFP-LC3-transfected MDA-MB-231 cells after overexpressing BRSK2 compared to those transfected with an empty vector, and exposed to a nutrient-deprived medium or not. As expected, nutrient starvation (6 h) significantly enhanced autophagosome formation (green puncta) compared with the control GFP-LC3-transfected MDA-MB-231 cells (Fig. 4C). As expected, BRSK2 overexpression significantly enhanced autophagosome formation in response to nutrient deprivation in MDA-MB-231 cells (Fig. 4C, quantification in D). Overexpression of BRSK2 marginally enhanced autophagosomes under normal growth conditions in MDA-MB-231 cells (Fig. 4C, D). Additionally, BRSK2 overexpression increased LC3-II levels and marginally elevated Beclin-1 protein levels in response to nutrient-deprived stress in MDA-MB-231 cells (Fig. 4E).

Next, we determine whether the BRSK2-induced increase of autophagosomes in response to nutrient deprivation stress reflected blocked downstream processing or elevated production of autophagosomes (increased flux)[72]. Downstream autophagosome processing involves fusion with lysosomes. Bafilomycin A1 (BafA1) prevents lysosomal acidification, thereby inhibiting autophagosome degradation[73]. An increase in LC3-

II levels in the presence of lysosomal degradation inhibitors is indicative of increased autophagic flux and LC3-II levels as a marker of autophagic flux stimulation[72,73]. Although higher LC3-II (cleaved and lipidated) levels and more GFP-LC3 puncta are observed in breast cancer cells engineered to overexpress BRSK2, we also measured autophagic flux and autophagosome number in the presence and absence of BafA1.

Our data suggested that ectopic expression of BRSK2 enhances autophagic flux and autophagosome numbers in breast cancer cells under nutrient-deprived stress (Fig. 5A–F).

As reported earlier for other cell models[31,38], we found that nutrient deprivation stress enhanced BRSK2 protein and BRSK2 mRNA levels in breast cancer cells (Fig. S6A, B), suggesting that environmental stress regulates BRSK2 expression. Epigenetic modifications may contribute to the transcriptional changes upon nutrient deprivation in cancer cells involved in autophagy[74,75]. The BRSK2 gene promoter has been implicated in being epigenetically silenced in cancers[76]. Hypoxic stress or epigenetic signaling enhances promoter histone modifications and promotes positive transcription of gene expression[77]. We found that both hypoxia (data not shown) or epigenetic drugs (suberoylanilide hydroxamic acid (SAHA) or 5-azacytidine) can re-express the *BRSK2* gene in breast cancer cells (Fig. S6B, C). Our data suggest that BRSK2 expression enhances autophagy in breast cancer cells in response to nutrient stress, thereby supporting breast cancer cell survival.

Inhibition of BRSK2 expression or its kinase activity reduces nutrient deprivation stress-mediated autophagy, cell growth, and survival, and enhances apoptosis of breast cancer cells

Autophagic signaling has a dual role in cancer cells. The autophagic process enhances cell survival signals in response to environmental stress. In contrast, in severe cellular stress conditions, such as tumor cells exposed to chemotoxic agents or massive deprivation of nutrients, uncontrolled autophagy occurs, which can proceed as an alternate autophagic cell death pathway by apoptosis[78]. In agreement with the data indicating that overexpressing BRSK2 enhances autophagy to protect cells from nutrient stress and is involved in cancer cell growth and survival, we assessed cell signaling pathways related to autophagy by downregulating BRSK2 in human breast cancer cells using siRNA targeted to human BRSK2. Figure 6 demonstrated that siBRSK2 markedly downregulated endogenous BRSK2 protein vs. control siRNA in MDA-MB-231 (Fig. 6A, B), BT-474 (Fig. 6C, D), and T-47D human breast cancer cells (Fig. S7). BRSK2 knockdown drastically downregulated several critical survival signaling pathways, including the AKT, ERK1/2, STAT3, and NF-κB pathways, in breast cancer cells (Fig. 6A).

Moreover, the downregulation of BRSK2 markedly reduced active LC3-II protein in MDA-MB-231, BT-474, and T-47D breast cancer cells (Fig. 6A–D, Fig. S7) or some of the other key proteins involved in the process of autophagy[14,22,79,80], including p62/SQSTM1, ATG3, or Beclin-1 in MDA-MB-231 cells (Fig. 6A). Strikingly, BRSK2 overexpression in knockdown cells rescued downregulated LC3-II protein (Fig. 6B, D, and Fig. S7) and the P-AKT (S473) level (Fig. 6B, D), strongly supporting that BRSK2 is an important regulator of autophagy and a cell survival factor in breast cancer cells. Interestingly, the downregulation of BRSK2 with siRNAs targeted to different target sequences of the human BRSK2 gene markedly reduced LC3-II protein levels in response to the nutrient stress in BT-474 breast cancer cells (Fig. 6C). These data suggested that endogenous BRSK2 kinase regulates autophagy and cell survival signaling pathways in breast cancer cells.

To further strengthen our data, we used another human TNBC cell line, BT-549, which has the highest expression of BRSK2. Downregulation of BRSK2 with siRNAs targeted to the endogenous BRSK2 significantly reduced BafA1-mediated elevated LC3-II protein levels and GFP-LC3 puncta (Fig. 7A, D and E). Similar attenuated autophagy data targeting BRSK2 with siRNA to BRSK2 in response to nutrient starvation and BafA1 exposure were also obtained in other cell lines, MDA-MB-231 (Fig. 7B) and BT-474 cells (Fig. 7C). Bafilomycin A1 (BafA1) is an autophagy inhibitor that can affect cell viability depending on the concentration and cell type. At nanomolar concentrations, BafA1 usually suppresses cell growth and triggers cell death, often by impairing autophagy flux. Our data suggested that siBRSK2 results in fewer viable cells in breast cancer cells in response to BafA1treatment. Since BRSK2 can protect cells under stress, the knockdown of BRSK2 sensitizes cells to reduced cell viability (Fig. S8).

In pancreatic ductal adenocarcinoma (PDAC) cells, BRSK2 expression results in AKT activity, cell growth, and survival via repressing mTORC1 through direct phosphorylation of TSC2 by BRSK2 serine/threonine kinase[34]. Next, we examine whether knocking down endogenous BRSK2 enhances apoptosis in response to nutrient stress in breast cancer cells. Using cell culture experiments, knocking down BRSK2 with siRNA targeted to human BRSK2 enhances cleaved PARP, Caspase-7, and -9, as well as cytochrome c release from mitochondria into the cytosol in response to nutrient stress in BT-474 (Fig. 8A) and MDA-MB-231 cells (Fig. 8B), as determined by immunoblotting with anti-cytochrome c as described previously[81,82].

As expected, siBRSK2 vs. control siRNA significantly reduced endogenous BRSK2 protein and the LC3-II protein levels in response to nutrient stress in these cells (Fig. 8A, B).

BRSK2 overexpression has been demonstrated in enhancing the phosphorylation of AMPK substrate proteins, autophagy proteins ULK1(S317), and p62(S351) in HEK293 cells, and a potent inhibitor of BRSK2, GW296115, was found to inhibit BRSK2-induced phosphorylation[35,36]. As shown in Fig. 8C (left and right) and Fig. S9A, B, GW296115 markedly reduced autophagy and autophagosome formation as demonstrated by reducing LC3-II levels and GFP-LC3 puncta staining in response to nutrient deprivation stress in MDA-MB-231 cells. Strikingly, GW296115 significantly reduced TNBC cell growth, 3D cancer cell invasiveness, and enhanced apoptosis as measured by cleaved caspase 7 and cleaved PARP in MDA-MB-231 cells (Fig. 8C–E). Furthermore, BRSK2 inhibition markedly reduced cancer cell colony formation and cell migration, as measured by the scratch/wound assay in MDA-MB-231 cells (Fig. S10A–E), further supporting its role in the autophagy, cell survival, and tumor metastasis processes.

To gain further insights into how BRSK2 regulates survival signals, such as AKT and autophagy, we knocked down AKT and BRSK2 individually and in combination to determine whether reducing autophagy

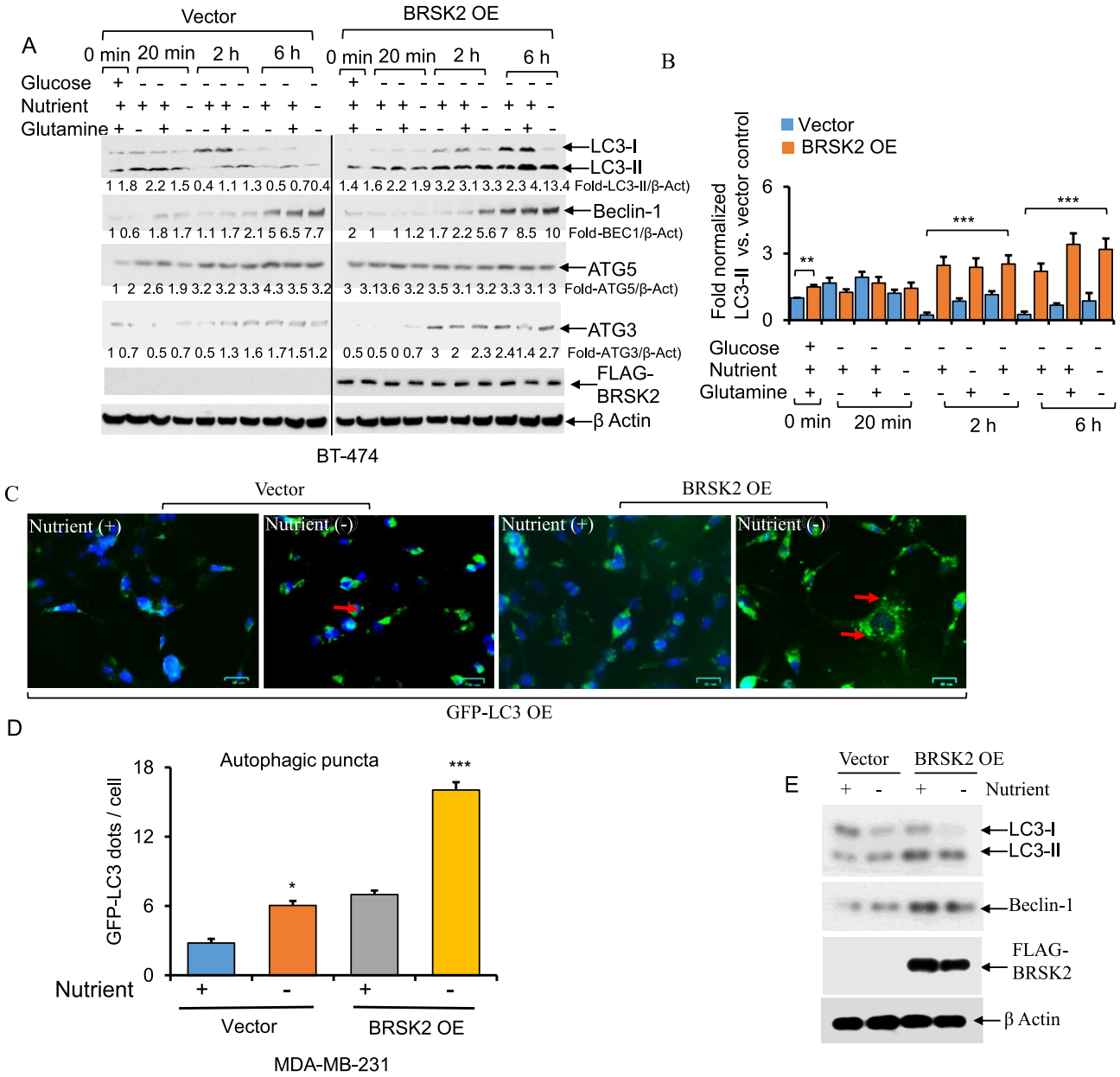

(as measured by LC3-II levels) affects tumorigenic properties in the TNBC cell model. Strikingly, siAKT1 and siBRSK2 in combination appeared to downregulate LC-II levels more than individual knockdown siRNA settings. Interestingly, individual siAKT1 or siBRSK2 significantly decreased 3D TNBC cell growth, and further, in combination with both siRNAs, have drastically reduced cell growth in 3D settings (Fig. S11A, B, E, and F).

We also knocked down ATG7[83] and BRSK2 individually and in combination with both siRNAs to show that the reduction of autophagy reduced tumorigenic properties in the TNBC cell model. Our data explained that targeting both autophagy by siATG7 and BRSK2 by siBRSK2 reduced autophagosome formation (LC3-II levels) and TNBC cell growth in 3D ex vivo cell modeling compared to individual knockdown (Fig. S11C, E, and F). Conversely, overexpression of BRSK2 in siAKT1 or siATG7[83] cells enhances LC3-II levels in these cells (Fig. S11D).

Additionally, a constitutively active AKT1 construct [myristoylated-(Myr)-Akt1][84] is utilized to examine whether gain of function (Myr-AKT) restores autophagy in siBRSK2 TNBC cell model, Constitutively active AKT1 (Myr-AKT1) marginally promotes LC-II levels; however, siBRSK2 drastically reduced LC3-II levels in these cells (Fig. S11G) and 3D cell growth (Fig. S11H) further suggesting BRSK2's role in autophagy linked to cell survival.

These data suggested that BRSK2 kinase increases autophagy in breast cancer cell models, resulting in tumor cell survival.

◀**Fig. 4**. Ectopic BRSK2 expression in breast cancer cells is associated with elevated autophagy in response to nutrient deprivation stress. (**A**) BT-474 cells were transfected with empty vector or BRSK2 overexpression plasmids for 48 h and subjected to exposure with various conditions with or without deprived energy sources medium (glucose, glutamine, or nutrients) for 0 h to 6 h, as indicated. Equal amounts of protein were used for Western blot analysis with autophagy-related protein antibodies. The total cell lysate was also analyzed by western blot, probed with an anti-FLAG antibody to reconfirm BRSK2 protein overexpression, and an anti-β-Actin antibody to confirm equal loading. (**B**) LC3–II band intensities (normalized to β-actin) were quantified by densitometry, and the measurements were used to calculate autophagy for each treatment separately (n = 4 independent experiments). BRSK2 overexpression increased autophagy in 6 h in response to nutrient-deprived stress. $^{**}p < 0.01$ and $^{***}p < 0.001$ (BRSK2 OE vs. corresponding empty vector control). (**C**–**E**) MDA-MB-231 cells were transiently transfected with either an empty vector or a green fluorescent protein (GFP)–tagged LC3 plasmid for 48 h, followed by an additional 6 h of nutrient starvation. (**C**) Microscopic images of autophagosome formation (puncta staining of GFP-LC3) and (**D**) quantification (puncta/cell) confirmed that BRSK2-mediated autophagosomes were increased within 6 h of nutrient starvation in MDA-MB-231 cells. During fluorescent microscopy, exposure time and weighting for GFP fluorescence were kept consistent between samples. Representative images (n = 10) were shown on a 25–27 μm scale bar. In addition, GFP-LC3 puncta staining was counted from at least n = 20 cells/sample to quantify autophagic puncta formation. Bar plots display data from autophagic puncta quantification assays, with means ± s.e. One-way ANOVA and post-hoc tests for pairwise comparisons are shown; $^{*}p < 0.05$, $^{***}p < 0.001$. (**E**) Similar experiments were performed in MDA-MB-231 cells exposed to ± nutrient-free medium for 6 h only, and total protein lysates were used for western blot analysis using the indicated antibodies. An anti-β-Actin antibody was used to ensure equal loading and transfer. For all western blotting experiments (n = 3), representative blots are shown. Fold LC3-II band and other autophagic protein band intensities normalized to β-Actin vs. control vector-transfected cells were labeled (ImageJ).

BRSK2 is in the Vps34-class III PI3K autophagy signaling complexes under nutrient deprivation stress in breast cancer cells

Class III PI3K Vps34 (vacuolar protein sorting 34) produces PI3P (phosphatidylinositol 3-phosphate; an inducer of autophagy) in the early endosomes in association with serine/threonine kinase Vps15 subunit and autophagy proteins ATG14 and Beclin-1 protein complexes involved in the progression of autophagy[85]. Next, we use CRISPR-Cas9-mediated BRSK*2* knockdown in the MDA-MB-231 cell model to assess endogenous BRSK2-mediated autophagy regulation and involvement of BRSK2 in the class III PI3K-autophagy protein complexes, respectively. To assess BRSK2 kinase-mediated autophagic protein complexes under nutrient deprivation stress, we have developed BRSK2 knockout transient overexpression models by transfecting the BRSK2 plasmid into MDA-MB-231 knockout cells compared to the empty plasmid. As shown in Fig. 9A, *BRSK2* knockout almost completely abrogated autophagy, as demonstrated by the reduction in LC3-II protein levels compared with the control cells. In agreement with our data, *BRSK2* knockout samples have reduced basal P-AKT (S473), phospho-NF-kB (S536), and other survival signaling molecules (Fig. 9A). BRSK2 knockdown cells have significantly reduced nutrient deprivation stress-mediated autophagic vacuoles and GFP-LC3 autophagic puncta (Fig. 9B, C). As expected, overexpression of BRSK2 in these knockout cells strikingly elevated autophagosome formation, as demonstrated by GFP-LC3 puncta staining (Fig. 9D). Nutrient deprivation-stress enhances class III PI3K Vps34 activity associated with autophagy protein complexes Beclin-1 and ATG14[85]. To elucidate the involvement of BRSK2-mediated autophagic signaling, we assessed changes in the BRSK2-mediated autophagy protein complexes in response to nutrient stress using immunoprecipitation (IP) of BRSK2. As shown in Figs. 10A and B, BRSK2 kinase associates with the basal levels of class III PI3K autophagy components (Vps34, Vps15, Beclin-1, and ATG14), and further, the association is markedly enhanced in response to nutrient deprivation stress in these cells. Our in vitro binding data confirmed that overexpressed FLAG-tagged BRSK2 directly interacts with overexpressed GFP-tagged ATG14 (Fig. 10C–E).

These data suggest a role for BRSK2 signaling, which controls autophagy to enhance Beclin-1, ATG14-associated class III PI3K complex in response to nutrient deprivation stress in cancer cells.

Endogenous BRSK2 is also associated with the class III PI3K-Vps34 autophagy protein complexes responding to nutrient-deprived stress in breast cancer cells (Fig. 10F).

Our data suggested that BRSK2 directly regulates autophagy associated with the components of the nutrient stress-induced class III PI3K autophagy machinery and cell survival (Fig. 10G).

Discussion

Autophagy is a cellular survival-promoting process in response to environmental stress, allowing cancer cells to adapt to nutrient deprivation and hypoxic stress[86,87]. Hypoxia/nutrient scarcity is a common feature of solid tumors like breast cancer due to the rapid growth of the tumors and an insufficient vascular network[88,89]. Although autophagy addiction occurs in breast cancer[90], how the autophagy-mediated catabolic system regulates tumor progression and metastasis is still unclear. The present study shows that BRSK2, the functional tumorigenic biomarker for aggressive metastatic breast cancer, is involved in tumor cell growth and survival and functions as an endogenous regulator of autophagy activation. BRSK2 expression is elevated under nutrient deprivation stress, and the elevated autophagosome levels induced by BRSK2 overexpression reflect increased autophagic flux. Interestingly, the protein kinase BRSK2 is associated with autophagy signaling protein complexes, which comprise the Vps34-class III PI3K, Beclin-1, and ATG14. It is involved in protecting breast tumor cells from nutrient deprivation stress through cell survival signals, such as PI3K/AKT, NF-κB, and STAT3.

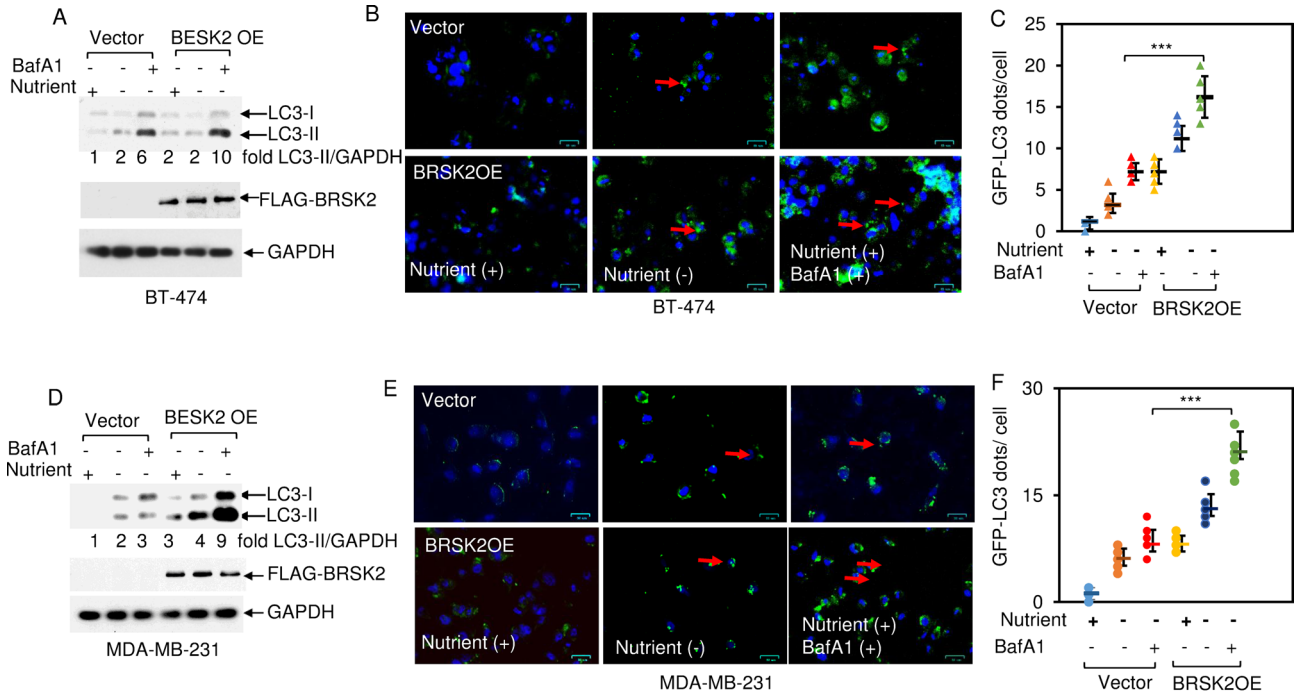

Figure 5

Fig. 5. BRSK2 overexpression enhances autophagy flux in breast cancer cells in response to nutrient deprivation stress. (**A**) BT-474 and (**D**) MDA-MB-231 cells were transfected with empty vector or BRSK2 overexpression plasmids for 48 h and subjected to nutrient-null medium ± BafA1 (100 nM) exposure for four h. Equal amounts of protein extracts from each sample were used for western blot analysis with the indicated antibodies—LC3, FLAG, and GAPDH—to ensure equal loading and transfer. Short and long-exposure FLAG-BRSK2 western blots were shown. n = 3, representative blots were shown. Fold LC3-II band intensities normalized to GAPDH vs. control vector-transfected cells were labeled (ImageJ). (**B, C,** and **E, F**) GFP-LC3 puncta staining and quantification. BT-474 (**B, C**) and MDA-MB-231 cells (**E, F**) were transiently transfected with either empty vector, BRSK2, or green fluorescent protein (GFP)–tagged LC3 plasmid for 48 h followed by an additional 4 h of nutrient starvation ± BafA1 (100 nM). (**B, E**) Microscopic images of autophagosome formation (puncta staining of GFP-LC3, red arrows) and (**C, F**) quantification (puncta/cell) confirmed that BRSK2-mediated autophagosomes were increased within 4 h of nutrient starvation in MDA-MB-231 cells. During fluorescent microscopy, the exposure time and GFP fluorescence weighting were kept consistent across all samples. Representative images (n = 10) were shown on a 25–27 μm scale bar. In addition, GFP-LC3 puncta were counted in at least n = 20 cells/sample to quantify autophagic changes. Scatter plots of data for autophagic puncta quantification assays are shown as means ± s.e., with one-way ANOVA and post hoc tests for pairwise comparisons; $^{***}p < 0.001$.

Our observations explain that BRSK2 expression is linked to AKT-mediated tumor cell survival, consistent with previous reports in PDAC[34]. Furthermore, the AMPK-subgroup kinases, e.g., BRSK2, have been implicated in autophagy processes[33].

Our data further revealed that *BRSK2* expression is highly upregulated in the primary tumors of breast cancer patients who have a history of metastasis compared to those without metastasis of TNBC patients. The BRSK2 transcript is upregulated in breast cancer tissues and cells compared to its absence in adjacent normal tissues or normal breast epithelial cells. In addition, BRSK2 protein and *BRSK2* mRNA levels are elevated in the lung-metastatic LM2-4 or the brain-metastatic MDA-MB-231BR compared with the parental TNBC MDA-MB-231 cells, suggesting its possible involvement in metastasis, as well as a predictive biomarker.

In agreement with a prior report[46], *BRSK1* may be silenced in human breast cancer cells. We also observed that the inflammatory TNBC SUM-149 cells have null BRSK2 protein expression (Fig. 2A). However, the *BRSK2* transcript is elevated (> threefold) in SUM-149 compared to MCF10A normal epithelial cells (Fig. 2B), suggesting a complex regulation of BRSK2. Previous studies reported BRSK2 protein degradation in the ubiquitin–proteasome pathway[47,48] and act extracellularly as an autoantigen in disease states[91], which elucidate yet uncharacterized physiological functions and molecular regulatory mechanisms of BRSK2 and BRSK1, and may partly explain the discrepancy between mRNA and protein expression in SUM-149 cells.

Our data revealed that in addition to the nutrient stress[34], epigenetic drugs such as TSA or 5-AZA markedly enhanced BRSK2 expression in breast cancer cells (Fig. S5). The solid tumor core is mainly composed of a hypoxic/nutrient-deprived stress environment that evokes an epigenetic signal that promotes the transcription

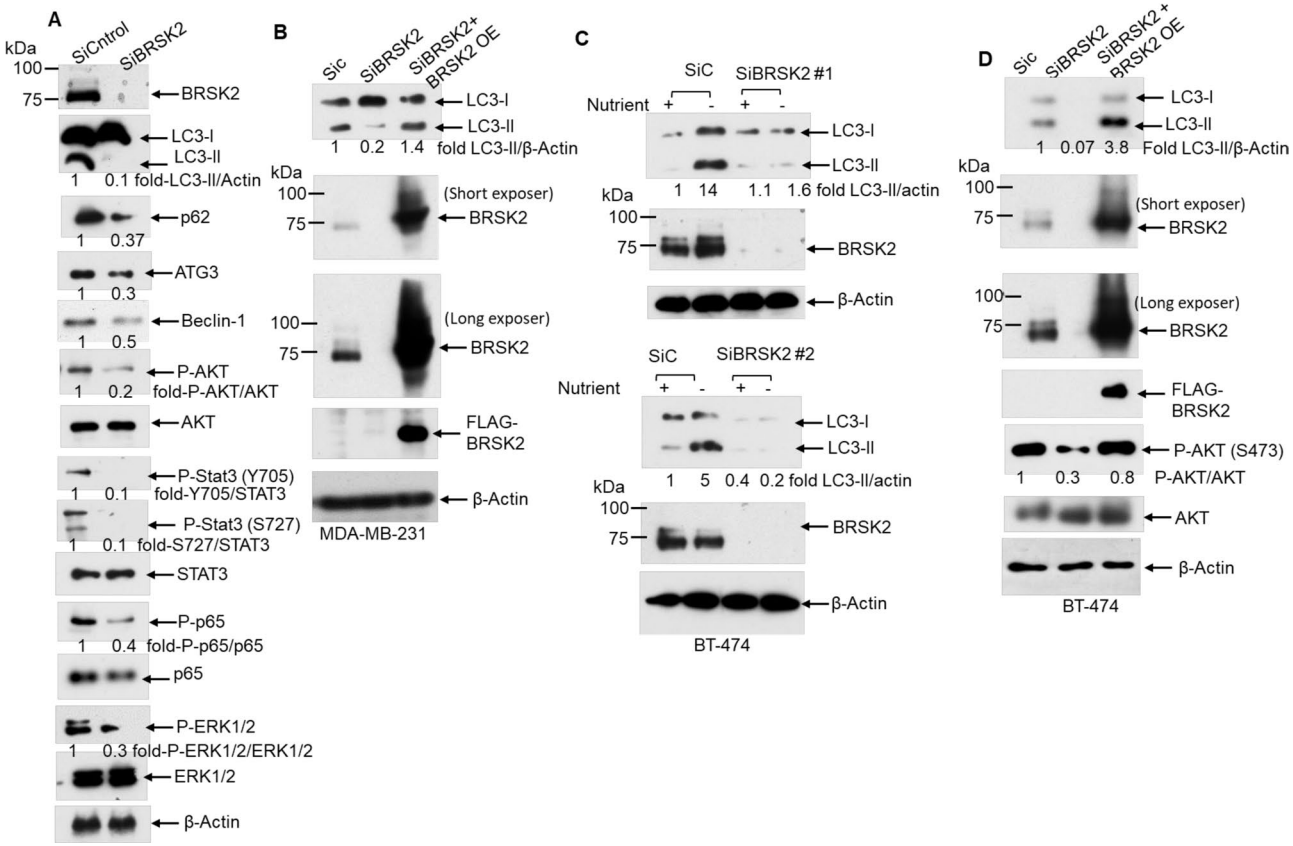

Fig. 6. Knockdown of BRSK2 suppresses AKT, STAT3, and NF-κB signaling, as well as basal autophagy and autophagy induced by nutrient deprivation stress, in breast cancer cells. (**A**) MDA-MB-231 cells transfected with siControl and validated siRNA targeted to BRSK2 were used for total protein lysate isolation, followed by western blot analysis with antibodies against the indicated proteins, including autophagy-related proteins p62/SQSTM1, ATG3, Beclin-1, active AKT (Ser473), STAT3 (Ser727 and Tyr705), phospho-ERK1/2, and NF-κB (Ser536). An anti-β-actin antibody was used to ensure equal loading and transfer. (**B**) BRSK2 is knocked down in MDA-MB-231 cells using siRNA targeted to BRSK2, compared to siControl. Knockdown of BRSK2 levels was rescued by ectopic overexpression of BRSK2. Equal amounts of total protein were used for Western blotting with antibodies against LC3, BRSK2, and FLAG-BRSK2. Short and long-exposure BRSK2 western blots were shown. β-Actin was used for equal loading and transfer. (**C**) BRSK2 protein was knocked down in BT-474 cells using two different siRNAs (siBRSK2 #1 and siBRSK2 #2) compared to siControl. Cells were exposed to ± nutrient-deprived medium for 6 h and subjected to total protein lysate isolation followed by western blotting. (**D**) BRSK2-knocked-down BT-474 cells with siRNA targeted to BRSK2 (siBRSK2 #1) ± rescued by overexpression of BRSK2 were used for total lysate isolation, followed by western blotting with antibodies against the indicated proteins, including BRSK2 and phospho-AKT. Short and long-exposure BRSK2 western blots were shown. β-Actin was used for equal loading and transfer. All western blotting experiments (n = 3) and representative blots are shown. Blots were scanned, and fold intensities normalized to respective loading control (β Actin) vs. vector control were labeled (ImageJ).

of genes associated with cancer progression and metastasis[75,92]. It could be possible that, similar to BRSK1[46], the BRSK2 gene remains turned off due to a methylated promoter and is expressed in response to specific environmental cues[93].

PI3K-AKT and the master transcription factors STAT3 and NF-κB are among the most potent tumor cell survival signaling pathways[50–56]. Indeed, the previous publication suggested a link between BRSK2 and AKT-mediated survival of pancreatic cancer cells[34]. Using the metastatic TNBC MDA-MB-231BR cell 3D spheroid model, we have demonstrated that expression of BRSK2 strongly activates AKT, STAT3, and NF-κB master survival signaling pathways. STAT3 activation by various growth factors and cytokines, including IL-6, requires phosphorylation at Tyr705 residue, mainly by Janus kinase 2 (JAK2). STAT3 is also subject to fine-tuning by other mechanisms, including serine (Ser727) and reversible acetylation. However, in human cancers, including breast cancer, STAT3 is often found to be constitutively activated[94]. NF-κB is also rapidly activated by proinflammatory cytokines, including IL-1β and TNF-α, and various cellular stresses, resulting in IκB phosphorylation and degradation, leading to nuclear translocation. Phosphorylation of p65-NF-κB at the Ser536 residue by IKKβ or other kinases is critical for NF-κB activation[95]. In addition to STAT3, NF-κB hyperactivity was also perceived in the resistance of chemotherapeutics or nutrient-deprived cellular stress via the downregulation of antisurvival

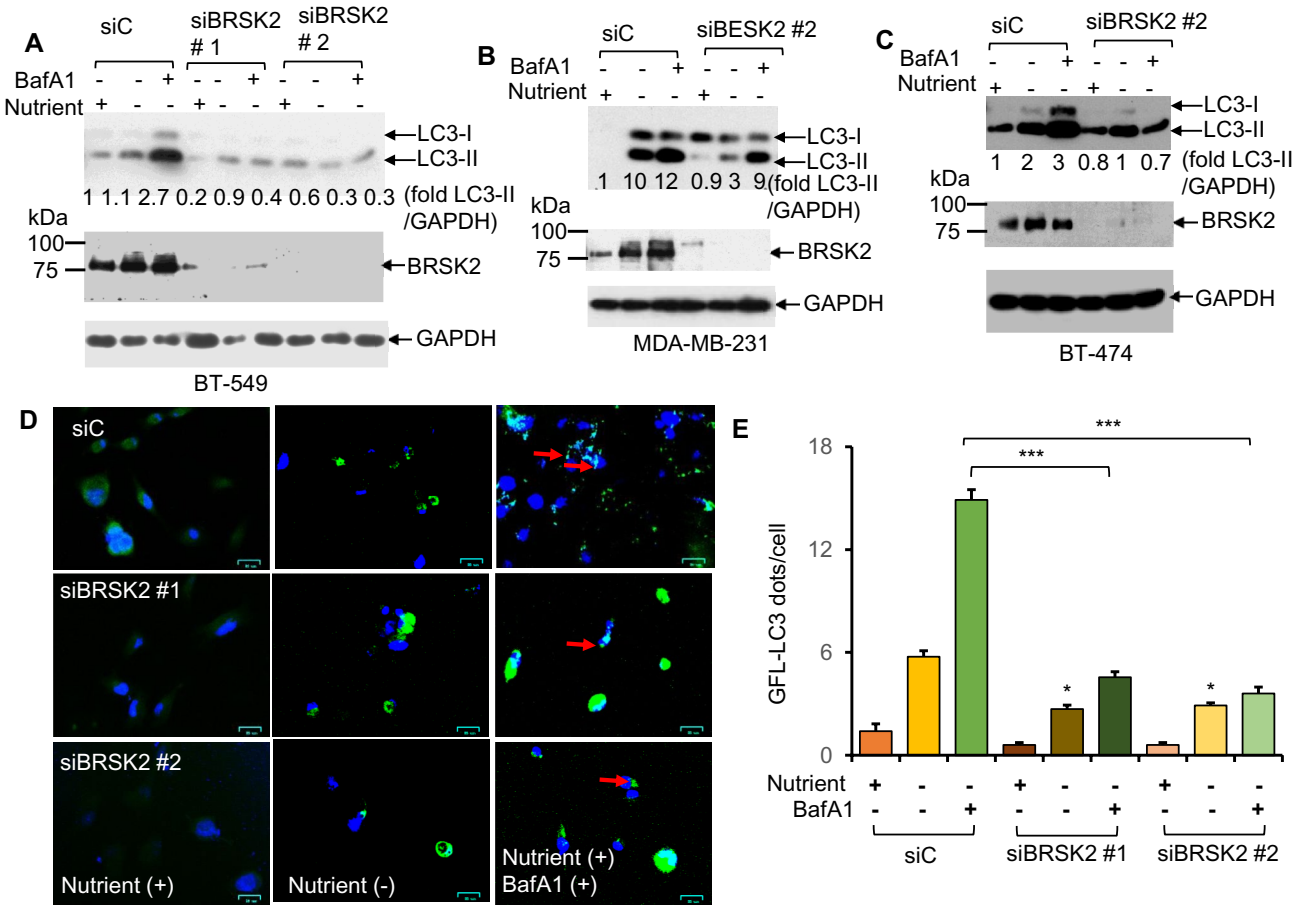

Fig. 7. BRSK2 downregulation reduces autophagy flux and autophagosome formation in breast cancer cells in response to nutrient deprivation stress and bafilomycin A1. (**A**) BT-549, (**B**) MDA-MB-231, and (**C**) BT-474 cells were transfected with siControl or siBRSK2 #1, or stBRSK2 #2 for 48 h and subjected to nutrient-null medium ± BafA1 (100 nM) exposure for 4 h. Equal amounts of protein extracts from each sample were used for western blot analysis with the indicated antibodies, including LC3, BRSK2, and GAPDH, as equal loading and transfer. N = 3, representative blots were shown. Fold LC3-II band intensities normalized to GAPDH vs. siControl transfected cells were labeled (ImageJ). (**D** and **E**) GFP-LC3 puncta staining and quantification. BT-549 cells were transfected with siControl, siBRSK2 #1, or green fluorescent protein (GFP)–tagged LC3 plasmid for 48 h followed by an additional 4 h of nutrient starvation ± BafA1 (100 nM). (**D**) Microscopic images of autophagosome formation (puncta staining of GFP-LC3, red arrows) and (**E**) quantification (puncta/cell) confirmed that siBRSK2-mediated autophagosomes were decreased within 4 h of nutrient starvation and BafA1 exposure in BT-549 cells. During fluorescent microscopy, the exposure time and weighting for GFP fluorescence were kept consistent across all samples. Representative images (n = 10) were shown on a 25–27 μm scale bar. In addition, GFP-LC3 puncta staining was counted from at least n = 20 cells/sample to quantify autophagic puncta formation. Autophagic puncta quantification assays are means ± s.e., one-way ANOVA, and post-hoc test for pair-wise comparison, $^{*}p < 0.05$ or $^{***}p < 0.001$ vs. siControl.

and upregulation of prosurvival target genes and pathways[96–98]. In 2010, Yoon S et al. demonstrated that STAT3 is activated by the reactive oxygen species (ROS) in nutrient starvation and enhances autophagy and inflammatory cytokines like IL6 in cancer cells[99]. We also observed that BRSK2-mediated activation of the transcription factor NF-κB markedly translocated to the nucleus in breast cancer cells.

Elevated levels of pro-inflammatory mediator expressions have been linked to tumor progression and metastasis[100]. Our data in tumor cells revealed that amino acid (glutamine) or nutrient deprivation markedly enhanced some of the cancer-associated key proinflammatory cytokines, such as IL-6, TNF-α, IL-1β, CCL5, and chemokines such as CXCL1, CXCL6, and CCL10, which are known to be regulated by NF-κB[62,101]. Interestingly, BRSK2 expression in breast cancer cells enhances some proinflammatory mediators. Although the autophagy and cytokine-chemokine regulations are still unclear in cancer[102,103], our data further provided a link between autophagy and metastasis mediator production (cytokines and chemokines) in tumor cells via BRSK2. Our data suggested that BRSK2 expression may promote breast cancer metastases via autophagy and pro-inflammatory mediator signaling[104,105]. However, further studies are required to decipher how BRSK2 signaling and increased autophagy cross-talk with survival signals, including transcription factors such as STAT3 and NF-κB.

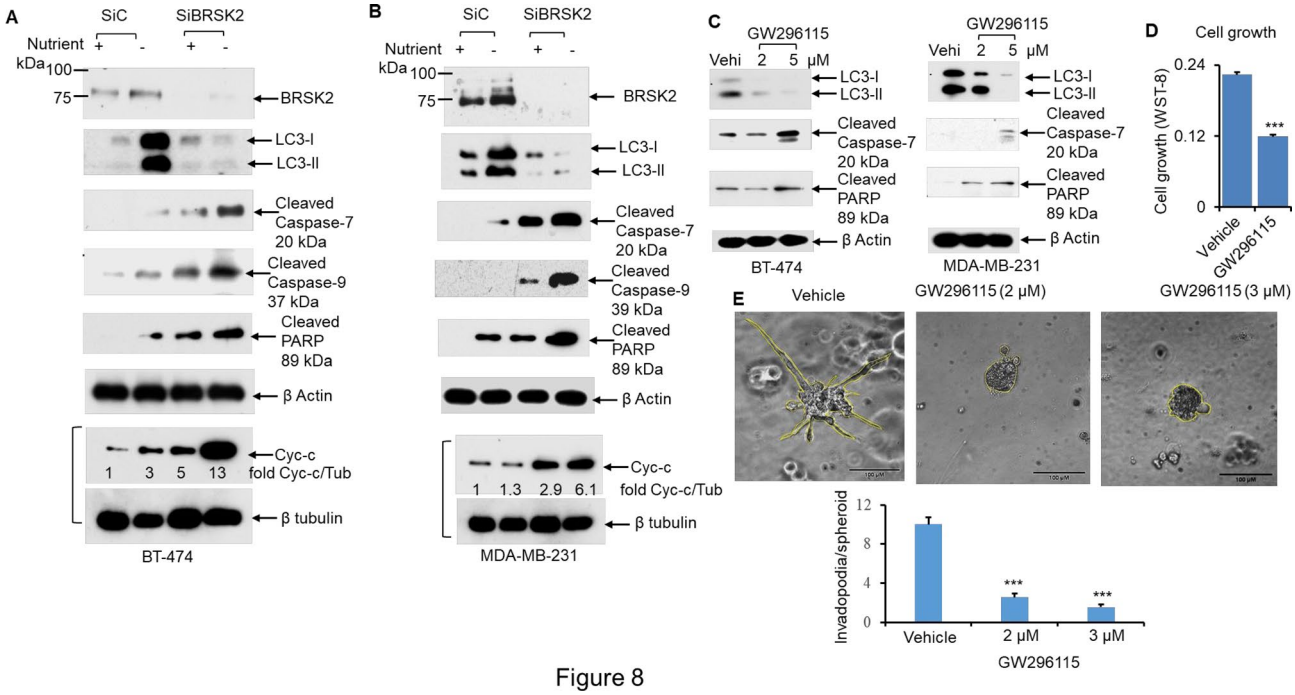

Figure 8

Fig. 8. Suppression of BRSK2 expression or inhibition by GW296115 reduces breast cancer cell growth and autophagy, thereby enhancing their apoptosis induced by nutrient deprivation stress. BT-474 (**A**) and MDA-MB-231 (**B**) cells were transfected with siRNA (Dharmacon, #1) targeted to BRSK2 or control siRNA for 48 h, and cells were exposed to ± nutrient-deprived medium for another 6 h, followed by total protein lysate isolation for western blotting analysis. BRSK2 downregulation efficiencies were validated by western blotting with anti-BRSK2 antibodies. Autophagy marker protein antibodies (anti-LC3) and apoptotic marker protein antibodies (anti-cleaved PARP, anti-cleaved caspase-7, and anti-cleaved caspase-9) were used, along with β-actin for equal loading. Proteins from duplicate cultures were resolved by SDS-PAGE, and cytochrome c released from mitochondria into the cytosol was assessed by immunoblotting using antibodies against cytochrome c (Cyc-c) and β-tubulin to ensure equal loading and transfer. Similar results were obtained in three additional experiments. All the apoptosis Western blots were also confirmed with siBRSK2 #2 (Qiagen, not shown). (**C**) Pharmacological inhibition of BRSK2, using GW296115 (2–5 μM) versus vehicle, decreased LC3-I/II protein levels but enhanced cleaved caspase. 7 and PARP proteins, as determined by western blotting in MDA-MB-231 cells. β-Actin was used as a loading control and for equal transfer. N = 3, representative blots were shown—similar data obtained in other breast cancer cells. All the blots were scanned, and fold intensities normalized to respective loading control vs. vector control were labeled (ImageJ). (**D**) Inhibition of BRSK2 kinase via GW296115 (2 μM) for 24 h reduced MDA-MB-231 cell growth, n = 5, Student's t-test, $^{***}p < 0.001$(GW296115 vs. vehicle control). (**E**) GW296115 (2–3 μM) vs. vehicle treatment for 72 h significantly reduced 3D Matrigel tumor cell invasiveness (invadopodia) in MDA-MB-231 cells. Representative light microscopic images (n = 10), scale bar 200 μm, quantification of invadopodia/spheroid, n = 10, ANOVA and post-hoc t-test, $^{***}p < 0.001$ vs. vehicle.

Tumor cell survival signaling pathways, including AKT, NF-κB, and STAT3, play complex roles in maintaining autophagy and are largely unexplored[106]. Particularly, the interplay between the PI3K/AKT pathway and autophagy can be complex and context-dependent. The PI3K α catalytic subunit inhibits autophagy, whereas its β catalytic subunit promotes autophagy in response to changes in ROS levels[107]. Under certain stress conditions, downregulation of P-AKT may not always lead to a compensatory increase in autophagy, potentially even resulting in a concurrent decrease in LC3-II (Fig. S11). To date, similar to AMPK, BRSK2 kinase is induced by nutrient starvation to inhibit mTOR by phosphorylating TSC2, promote autophagy, and recent studies suggest BRSK2 signaling leads to activation of PI3K/AKT signaling[33–36]. AKT can be involved in both upstream and downstream regulation of mTORC1[39]. Activation of mTORC1 strongly represses upstream PI3K/AKT signaling through a potent negative feedback loop and functions as a brake on AKT activation in cancer[40]. Therefore, in agreement, new studies showed that starvation-induced BRSK2 repression of mTOR may cause a loss of feedback inhibition on AKT activation, and ultimately, AKT is activated[34].

Our current study has some limitations. Bioinformatics methods and limited sample sizes in the patient databases are biased. We need to combine more database samples to screen more thoroughly and identify differences. We have conducted only in vitro experiments. In the future, we should conduct in vivo experiments to validate the analysis results further.

In conclusion, the study uses molecular biology, biochemistry, and pharmacological approaches to advance our understanding of the contribution of the dark kinome member, the serine/threonine protein kinase BRSK2,

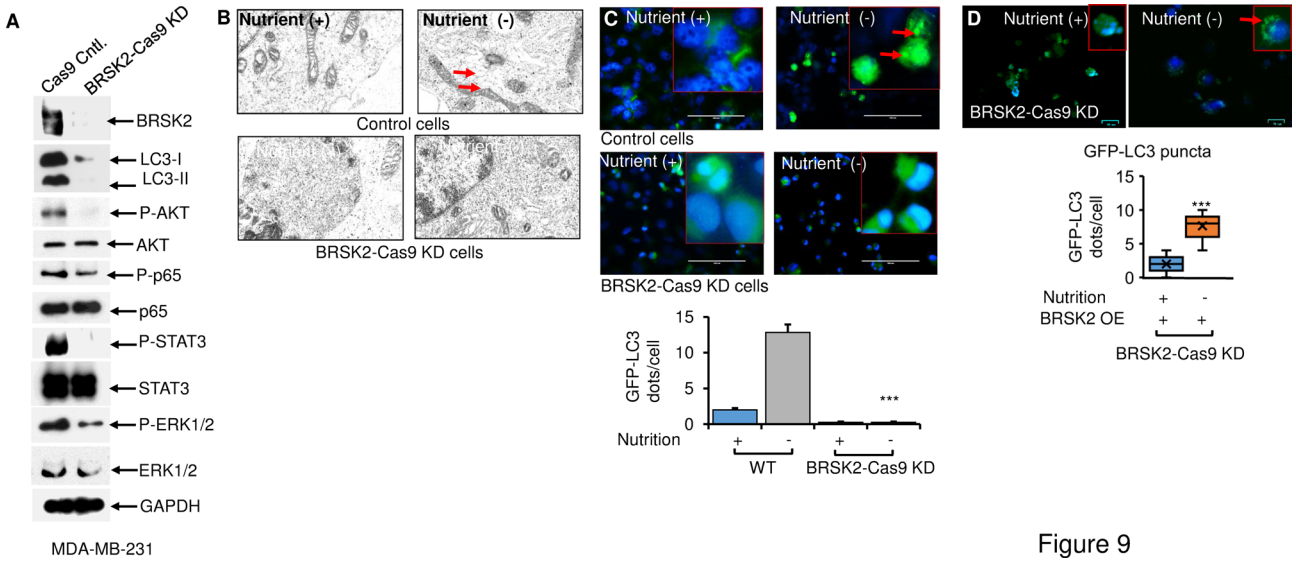

Figure 9

Fig. 9. BRSK2 is involved in nutrient deprivation stress-mediated autophagic vacuole formation. (**A**) The endogenous *BRSK2* gene was knocked down by CRISPR-Cas9 vs. CRISPR control in MDA-MB-231 cells, and a stable *BRSK2* knockout clone was selected and verified by western blotting with anti-BRSK2 antibodies. As expected, knockout cells have markedly reduced LC3-II levels, P-ERK1/2, P-AKT, and P-p65-NF-kB protein levels. GAPDH was used for equal loading and transfer in Western blotting. Experiments were repeated three times, and representative blots are shown. Blots were scanned, and protein bands were quantified (ImageJ). (**B**) *BRSK2* knockout MDA-MB-231 cells vs. control cells were exposed to ± nutrient-free medium for 6 h and subjected to TEM analysis, n = 10, representative image, scale bar 200 µm, and red arrows indicate autophagosome vacuoles. (**C**) Duplicate cells from (**B**) were transfected with GFP-LC3 and treated with or without nutrient-free medium for 6 h, followed by GFP immunofluorescence staining. Representative inverted fluorescence microscopic images, n = 10, scale bar 100 µm, red arrows on blowout images indicate autophagy puncta GFP-LC3 staining (n = 20 cells). ANOVA and post-hoc t-test, $^{***}p < 0.001$ vs. vehicle. (**D**) BRSK2 overexpression in knockout cells enhances autophagy in response to nutrient deprivation. BRSK2 was overexpressed in BRSK2 knockout MDA-MB-231 cells, followed by GFP-LC3 overexpression. Cells were then exposed to ± nutrient-free medium for 6 h and followed by GFP immunofluorescence imaging. Representative inverted fluorescence microscopic images were shown, n = 10, scale bar 100 µm, red arrows on blowout image, indicating autophagy GFP-LC3 puncta staining (n = 20 cells). Box plots are the number of dots/cells from at least n = 20 counted, Student's t-test, $^{***}p < 0.001$ (nutrient-free vs. nutrient plus medium). KD, knockdown.

as a predictive biomarker for aggressive metastatic diseases, and to elucidate its role in regulating autophagy, cell survival, and invasion in breast cancer. However, the major open questions still to be addressed in the study of BRSK2 are i) is there any proteins get phosphorylated in the autophagy complexes since it is a protein kinase; ii) is it playing any role in the phosphorylation of other proteins outside the autophagy complexes, which in turn play a role in survival signals; iii) How do autophagic cells after survival from stresses establish in distant organs.

Materials and methods

Cell culture and treatments

All the established cell lines, including human estrogen receptor-positive (ER +) breast cancer MCF-7 (HTB-22), BT-474 (HTB-20), T-47D (HTB-133), ZR-75-1 (CRL-1500), and triple-negative breast cancer (TNBC) MDA-MB-231 (CRM-HTB-26), BT-549 (HTB-122) and HEK293 (CRL-1573) cell were from American Tissue Culture Collection (ATCC)[75,108–111]. Inflammatory breast cancer (IBC) SUM-149 cells were provided by Dr. Mateusz Opyrchal (Indiana University School of Medicine, USA)[112]. TNBC lung-metastatic clone LM-2-4 cells of parental MDA-MB-231 cells, a generous gift from Dr. John Ebos [Roswell Park Comprehensive Cancer Center (RPCCC), USA][75,108,110]. Human TNBC, brain-metastatic clone MDA-MB-231BR of parental MDA-MB-231, was obtained from Dr. Patricia S. Steeg (National Cancer Institute, USA)[113]. All cells were cultured in Dulbecco's modified Eagle medium (DMEM; Gibco, 11965-092) containing 4500 mg/l D-glucose, 4 mM L-glutamine, and 110 mg/l sodium pyruvate, supplemented with 10% fetal bovine serum (FBS; Gibco, 16141079). Human breast epithelial MCF10A cells were kindly provided by Dr. Santosh Patnaik (RPCCC, USA)[110]. MCF10A cells were cultured in DMEM/F12 medium (Gibco, 11320-033) supplemented with 5% horse serum (Gibco, 26050088), 0.5 µg/ml hydrocortisone (Sigma, H0135), 100 ng/ml cholera toxin (Sigma, CB052), 10 µg/ml insulin (Sigma, 15500), and 20 ng/ml recombinant human epidermal growth factor (EGF; (Sigma, E5036). For glucose or glutamine starvation experiments, cells were washed with PBS (1X) and cultured in glucose-free DMEM (Gibco, 11966-025) or glutamine-free DMEM medium (Gibco, A14430-01) containing 10% dialyzed FBS (Gibco, A33820-01). For Nutrient starvation experiments, cells were rinsed and treated with EBSS medium (Gibco, 14155-63). For

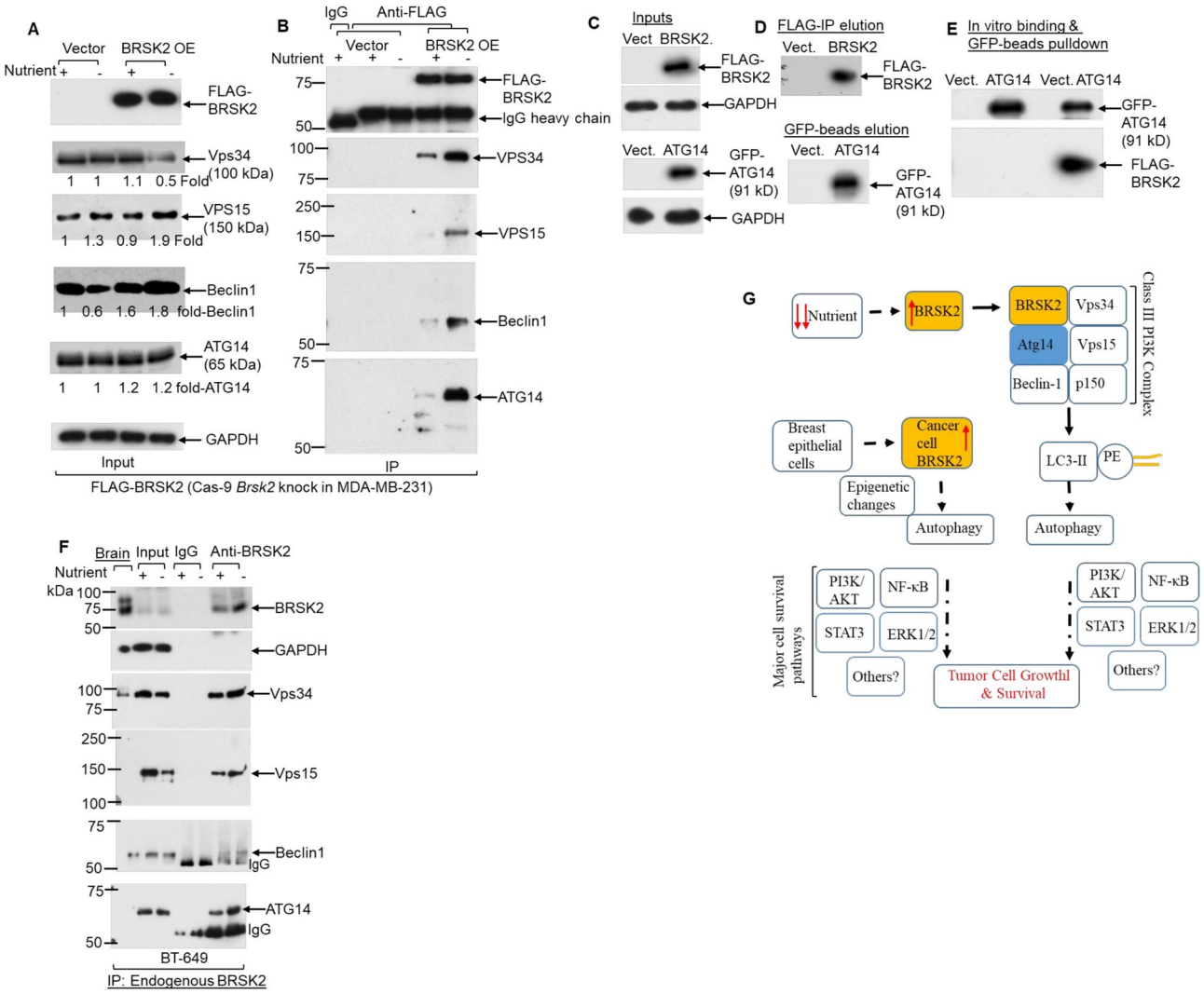

Fig. 10. BRSK2 is involved in the formation of the Vps34-class III PI3K-Beclin-1-ATG14 autophagy signaling complex. (**A** and **B**) BRSK2 was ectopically overexpressed in MDA-MB-231 *BRSK2* knockout cells. Vector-transfected control cells and BRSK2-overexpressed cells were exposed to a nutrient-free medium with or without nutrients for 6 h. As indicated, equal amounts of total cell lysate protein were immunoprecipitated with control IgG and anti-FLAG antibodies. Inputs (**A**) and immunoprecipitated BRSK2-protein complexes with anti-FLAG antibodies (**B**) were resolved in SDS-PAGE for western blotting with the indicated protein antibodies. Anti-FLAG antibodies were used to detect the FLAG-tagged BRSK2 protein. (**C**–**E**) BRSK2 interacts with ATG14 in vitro. (**C**) FLAG-BRSK2 and GFP-ATG14 were ectopically overexpressed in MDA-MB-231 cells with an empty vector. Equal proteins from cell extracts were used for western blot analysis (inputs) to demonstrate FLAG-BRSK2 (top panel) and GFP-ATG14 (bottom panel) protein expression in these cells. (**D**) 500 µg total proteins from each sample were used in FLAG-BRSK2 IP (top panel) and GFP-ATG14 GFP-beads pulldown (bottom panel) experiments. Eluted proteins from extensively washed FLAG-IP Protein G beads and pulldown GFP beads were used for western blots and subjected to in vitro binding and western blot analysis, as indicated (**E**). FLAG-IP eluted proteins (vector and BRSK2) were separately incubated with the GFP-beads eluted proteins (Vector and ATG14) for 30 min at room temperature. GFP-bead pulldown captured GFP-tagged ATG14 and bound BRSK2 and was analyzed by Western blot with the indicated antibodies. (**F**) With or without nutrient-starved (6 h) BT-549 cells, equal protein amounts were incubated with anti-BRSK2 or control IgG antibodies to immunoprecipitate endogenous BRSK2 protein complexes. Input proteins and anti-BRSK2 immunoprecipitated protein complexes were resolved in SDS-PAGE for western blotting with the indicated protein antibodies. A whole-mouse-brain protein extract (1/10th of the input) was used as a positive control for BRSK2. GAPDH was used to load and transfer the input samples equally. Western blots (n = 3) and representative blots are shown. (**G**) We propose that BRSK2-mediated autophagy and tumor cell survival signaling in response to nutrient-rich or nutrient-deprived stress involve the class III PI3K-Vps34-Beclin-1-ATG14 pathway in breast cancer cell models.

some experiments, cells were exposed to EBSS ± 100 nM bafilomycin A1 (Cell Signaling, 54645) for 4 h or 24 h and processed for molecular analysis.

Transfection

BRSK2 (RC223466) expression plasmid was purchased from OriGene Technologies. BRSK1 (66881) expression plasmid was purchased from Addgene (deposited by Dr. Maria Alvarado-Kristensson, Lund University, Sweden).

EGFP-LC3 (11546) was purchased from Addgene (deposited by Dr. Karla Kirkegaard, Stanford University, USA). Following the manufacturer's instructions, cells were transfected with BRSK2 and BRSK1 plasmids, as well as control plasmids, using the Lipofectamine P3000 transfection kit (Invitrogen, L3000-015). Using a GFP control plasmid and Lipofectamine P3000 for transfection, we found that the transfection efficiency was greater than 70% for all cell lines tested in our studies.

For the Autophagosome formation assay, MDA-MB-231 cells were plated at 60% confluency the day before transfection. On the day of transfection, cells were washed with PBS (1X) and transfected with EGFP-LC3 with Lipofectamine 3000, following the manufacturer's instructions. After 24 h of transfection, cells were again transfected with the BRSK2 plasmid (0.75 µg/well; 1×10^6 cells) and empty vector (OriGene, PS100001). After 24 h of BRSK2 transfection, the cells were washed, fixed with formalin, and used for fluorescence microscopic imaging. Images were acquired and processed with the ZOE Fluorescent Cell Imager (Bio-Rad, USA). For some experiments, GFP-LC3 images were acquired by the EVOS FL imaging system (Life Technologies, USA). BRSK2 expression in various human breast cancer cells was down-regulated by transfection with sequence-specific small interfering RNA (siRNA) for human BRSK2.

siBRSK2 #1: ON-TARGETplus SMARTpool siRNA against BRSK2 (L-005381-00) and ON-TARGETplus Non-targeting Control Pool (D-001810-10) from Dharmacon were used to confirm the lack of off-target effects—ON-TARGETplus SMARTpool siRNA BRSK2 target sequences: 5′-UAAGGAGGCUCGGAAGUUC-3′; 5′-GAUCUUCGUGGUCAUCAAA-3′; 5′-GGCCAGCCGUGUUCCAGAA-3′; 5′-AGAAUGAGCCCGAA CCAGA-3′. siBRSK2 #2: Qiagen human siBRSK2 (sense, 5′-CUUCGACGAUGACAACUUGTT-3′; 5′-CAAG UUGUCAUCGUCGAAGTT-3′) and control siRNA (Qiagen, USA) using Oligofectamine (Invitrogen, 12252-011). For some experiments, we have used siControl (Dharmacon) as a control for siBRSK2 #1 and siBRSK2 #2. siControl from Dharmacon and siControl from Qiagen have similar cellular responses to naïve untreated siRNA cells. In addition, siAKT1: ON-TARGETplus siRNA against human AKT1 (J-003000-10), target sequence: 5′-C AUCACACCACCUGACCAA-3′; siATG7: ON-TARGETplus siRNA against human ATG7 (J-020112-06), target sequence: 5′-GAUCUAAAUCUCAAACUGA-3′ from Dharmacon were used for some experiments.

As recommended, Oligofectamine (Invitrogen), a reagent used for siRNA transfection, can achieve transfection efficiencies ranging from 50 to 97% in various cancer cell lines.

Immunoblotting, immunoprecipitation, and pulldown

Cultured breast cancer cells were washed twice with the ice-cold 1X PBS and lysed by probe-sonication in the lysis buffer containing 20 mM Tris–Cl (EMD Millipore, 648310), pH 7.4, 20% glycerol (Sigma, G5516), 150 mM NaCl (Fisher, BP358), 0.5% NP-40 (Thermo Scientific, 85124), 5 mM sodium orthovanadate (Sigma, S6508), 40 mM β-glycerophosphate (Sigma, G9422), 15 mM NaF (Sigma-Aldrich, 450022), 0.5 mM 5-Deoxypyridoxine hydrochloride (Sigma, D0501), and protease inhibitor cocktail (Sigma, 539136). Unbroken cells were removed by centrifugation at 700 × g for 10 min at 4 °C. Protein concentrations were measured by the Bradford method (Bio-Rad, 5000006). Immunoblotting: A total of 25 µg of protein was loaded per lane, separated by 10% SDS-PAGE, and transferred to nitrocellulose membranes. Membranes were blocked with 5% blocking solution in 1X TBST buffer (Bio-Rad, 170-6435) at room temperature (RT) for 1 h. Membranes were incubated overnight at 4 °C with the respective primary antibodies (1:1000 dilution) in TBST buffer. After hybridization with primary antibodies, membranes were washed thoroughly with TBST buffer at room temperature, followed by incubation for 1 h at RT with the respective secondary antibodies (1:5000 in TBST with 1% blocking solution; Bio-Rad, 1706404). Membranes were washed thoroughly at RT and developed with the enhanced chemiluminescence (ECL) western blotting substrate (Pierce, 32106). Western blot images were obtained by exposing the membranes to X-ray films (Thermo Scientific, 34091). The following primary antibodies were used for western blot analysis: anti-BRSK2 (#11589-1-AP) from Proteintech, USA. β-Actin (4970), BRSK1 (5935), phospho-AKT (Ser473; 4060), total AKT (4685), LC3I/II (13082), p62/ SQSTM1 (39749), ATG3 (3415), ATG5 (12994), ATG7 (8558), ATG14 (96752), Beclin-1 (3495), vps34 (PIK3C3, 3358), vps15 (PIK3R4, 14580), phospho-ERK1/2 (Thr202/Tyr204; 9524), ERK1/2 (4695), phospho-NF-κB p65 (Ser536; 3033), NF-κB p65 (8242), phospho-STAT3 (Y705; 9145), phospho-STAT3 (Ser727; 34911), STAT3 (9139), Histone H3 (4499), Cytochrome c (11940), Cleaved caspases-7 (8438), cleaved caspase-9 (20750), cleaved PARP (5625), Glyceraldehyde-3-phosphate dehydrogenase (GAPDH; 5174), β-Tubulin (2146) are from Cell Signaling Technology, USA. α-Tubulin antibody (T6199) is from Sigma-Aldrich, USA. Clathrin Heavy Chain (CHC; sc-58714), Lamin B1 (sc-365962), and β-Actin (sc-47778) are from Santa Cruz Biotechnology, USA. The following secondary antibodies were used for western blot analysis: peroxidase-conjugated affipure goat anti-rabbit IgG (111-035-045) and goat anti-mouse IgG (115-035-062) are from Jackson Immuno-Research Laboratories, USA. All the antibodies used in this manuscript are specific to the respective proteins (LC3-I/II, Beclin1, ATG3, ATG5, ATG7, ATg14, p62, Vps34, Vps15, FLAG, GFP, HA, AKT total, phospho-AKT, ERK1/2 total, phospho-ERK1/2,p65 total, phospho-p65, STAT3 total, phospho-STAT3, cleaved caspase-7, -9, -cleaved PARP, cytochrome –C, BRSK2, BRSK1, GAPDH, CHC, α tubulin, β tubulin, β actin, Histone H3, and Lamin B1) have been optimized experimentally in the laboratory for obtaining single-band detection without visible edge of the blots using the X-ray film development method. The blots were cropped prior to hybridization with the respective antibodies, as mentioned in the Figures & Legends. A portion of the full-length blots of the original blots was provided in Supplementary Figure S12.

Immunoprecipitation and pulldown: Total protein extracts isolated from empty vector-transfected MDA-MB-231 cells or BRSK2-Cas-9 knockout MDA-MB-231 cells (see below), which were transfected with FLAG-BRSK2 and treated with or without a nutrient-free medium, were immunoprecipitated using monoclonal anti-FLAG M2 antibody (Sigma-Aldrich, F3165) or control normal IgG (Santa Cruz, sc-2025). For endogenous BRSK2 immunoprecipitation, 500 µg total proteins from BT-549 cells treated with or without a nutrient-free medium (6 h) were immunoprecipitated with antibodies against anti-BRSK2 antibodies (#11589-1-AP, Proteintech, USA) or control normal IgG. Immunoprecipitates were captured with protein A/G PLUS-Agarose beads (Santa Cruz, sc-2003). After washing the beads four times with lysis buffer, the bound proteins were released by boiling in sodium dodecyl sulfate–polyacrylamide gel electrophoresis (SDS-PAGE) sample buffer and analyzed by Western blotting. For some experiments, GFP-ATG14 (Addgene, #24295) transfected cell extracts were used for GFP-agarose pulldown (Proteintech, #gta) experiments[114]. For in vitro binding experiments, pulldown or immunoprecipitated proteins were eluted using a low-pH glycine buffer and immediately neutralized by the tris buffer.

CRISPR/Cas9 technology targeting human BRSK2 and a stable cell line

CRISPR/Cas9 technology was utilized to knock out the BRSK2 gene in the human breast cancer MDA-MB-231 cells. Human CRISPR/Cas9 guide RNA(gRNA) guides were designed based on the human BRSK2 gene (GenBank accession number: NM_001256627.2). To knock out human BRSK2 in MDA-MB-231 cells, 2 sgRNA sequences were designed using the CRISPR algorithm (CRISPR (tefor.net)). The guide sequences were as follows: CTCACGGTTGACGATCTTGATGG and TCACTGCGTCACCTGCCAGAAGG. The crRNA and trRNA were purchased from IDT (Integrated DNA Technologies, USA) and resuspended to 160 µM each. crRNA and trRNA (1:1) were complexed by a touchdown PCR method (Alt-R ordered from IDT), and Cas9 3NLS protein was added to make a functional ribonucleoprotein (RNP). RNP was added to 3×10^6 cells suspended in Opti-MEM media (Gibco, 11058021). The cell mixture was then electroporated under optimized conditions using a NEPA21 electroporator (Nepa Gene, Japan) and subsequently transferred into 6-well plates containing 2 mL of complete medium without antibiotics. Three days after transfection, cells were treated with 2 µg/ml of puromycin (Sigma-Aldrich, P8833). After three weeks of selection with 2 µg/ml puromycin, the verified clones were identified using immunoblot analysis and subsequently cultured in maintenance medium containing 0.5 µg/ml puromycin. Stable MDA-MB-231 cells were named Control cells and BRSK2-Cas9 KD cells, respectively. For some experiments, BRSK2 was ectopically overexpressed in BRSK2-Cas9 KD cells compared to empty vector-transfected control cells. These cells were then exposed to ± nutrient-free medium for total protein extractions for further studies.

Real-time PCR

Quantitative real-time PCR (qPCR) analysis was performed as described before[75,109,114,115]. Briefly, total RNA was prepared with Trizol from cultured cells or tissue specimens from breast cancer patients (Invitrogen, 15596-018). Human breast tissue specimens were ground into a fine powder in liquid nitrogen without thawing and suspended in Trizol before isolating the total RNA. DNA contamination was removed from RNA with DNase treatment (Qiagen, 79254). RNA (2 µg) was reverse transcribed with the high-capacity cDNA Archive kit (Applied Biosystems, 4368814). cDNAs were diluted tenfold (target genes) and 100-fold *GAPDH* (house-keeping gene), and qPCR was performed using SYBR Green PCR Master Mix (Thermo Scientific, K0251) on CFX96 cycler (Bio-Rad, USA). Gene expression levels were calculated using the 2 – (ΔΔCT) method (49, 50) and normalized to *GAPDH* expression. The following real-time PCR primers for human genes are used in this manuscript, *BRSK2*-F: 5′-CGACGATGACAACTTCGCAC-3′, *BRSK2*-R: 5′-ATGCCCCGTACGAGACTCT-3′; *BRSK1*-F: 5′-TATGCGTGTCCAGAGGTGATT-3′, *BRSK1*-R: 5′- GGAGGTTGTCGTCATCAAAGG-3′; *GAPDH*-F: 5′-CTTAGCACCCCTGGCCAAG-3′, *GAPDH*-5′:GATGTTCTGGAGAGCCCCG-3′; *CXCL10*-F: 5′-GTGGCA TTCAAGGAGTACCTC-3′, *CXCL10*-R: 5′-TGATGGCCTTCGATTCTGGATT-3′; *CCL5*-F: 5′- CCAGCAGT CGTCTTTGTCAC-3′, *CCL5*-R: 5′-CTCTGGGTTGGCACACACTT-3′; *IL6*-F: 5′GAG GCA CTG GCA GAA AAC AA-3′, *IL6*-R: TGG CAT TTG TGG TTG GGT CA-3′; *IL8*-F: 5′- AGG TGC AGT TTT GCC AAG GA-3′, *IL8*-R: 5′- TTT CTG TGT TGG CGC AGT GT-3′; *CXCL1*-F: 5′-GCCAGTGCTTGCAGACCCT-3′, *CXCL1*-R: 5′- GGCTATGACTTCGGTTTGGG-3′; *TNFα*-F: 5′-AGCCCATGTTGTAGCAAACC-3′, *TNFα*-R: 5′-TGAGG TACAGGCCCTCTGAT-3′; *IL-1β*-F: 5′-GGACAAGCTGAGGAAGATGC-3′, *IL-1β*-R: 5′-TCGTTATCCCATG TGTCGAA-3′; *CXCL6*-F: 5′-AGAGCTGCGTTGCACTTGTT-3′, *CXCL6*-R: 5′- GCAGTTTACCAATCGTTTT GGGG-3′; *CXCL2*-F: 5′-GCCAGTGCTTGCAGACCCT-3′, *CXCL2*-R: 5′-GGCTATGACTTCGGTTTGGG-3′; *AKT1*-F: 5′-TGGACTACCTGCACTCGGAGAA-3′, *AKT1*-R: 5′-GTGCCGCAAAAGGTCTTCATGG-3′.

Nuclear protein extracts

Nuclei-free cytoplasmic and nuclear fractions were isolated from BT-474 and MDA-MB-231 cells using a low-salt extraction procedure previously described[114,116]. In brief, PBS washed cells were resuspended in low-salt buffer A containing 10 mM of HEPES (Sigma-Aldrich, H4034), pH 7.8, 10 mM of KCl (Sigma-Aldrich, P5405), 0.1 mM of EDTA (Sigma-Aldrich, E8008), 1 mM of Na3VO4, 1 mM of DL-Dithiothreitol (DTT; Sigma-Aldrich, D0632), 0.2 mM of PMSF (Sigma-Aldrich, 93482), and 1:500 protease inhibitor cocktail (Sigma-Aldrich). Cell pellets were ground into a fine powder in liquid nitrogen without thawing and suspended in ice-cold buffer A. Cell powder suspensions in buffer A were incubated for 15 min on ice, followed by vortexing for 10 s at RT with NP-40 (final concentration 0.75%), and then incubated on ice for another 2 min. Crude nuclei pellets and nuclei-free cytoplasmic fractions were separated by centrifugation at 850 × g for 3 min at 4 °C. Nuclear pellets were washed twice with two volumes of buffer A. Nuclei were then dissolved in a high salt buffer containing 20 mM HEPES, pH 7.8, 0.4 M NaCl, 1 mM EDTA, 1 mM Na3VO4, 1 mM DTT, 0.2 mM PMSF, and 1:500 protease inhibitors cocktail and incubated on ice for 15 min. Nuclear extracts were isolated by centrifugation at 14,000 × g for 5 min at 4 °C.

3D cell culture and invasiveness assay

Cancer cell spheroid assays were performed as described previously[75,110,117,118]. Briefly, 20,000 cells were transfected with either the control expression vector or BRSK2 or BRSK1, as mentioned above in the transfection section. After 24 h of transfection, cells were mixed thoroughly with the Matrigel (Corning, 354234)(60:40% ratio) and cultured in DMEM F12 medium (Gibco) supplemented with 20 ng/ml each of human EGF (Sigma), human FGF (PeproTech, 100-18B), and 1X B27 (Gibco, 17504-044) in ultra-low attachment 24-well plates (Corning, 3473) for 48 h. Spheroids were then collected, and proteins were extracted for Western blot analysis. For Drug treatment, 20,000 MDA-MB-231 cells were mixed with Matrigel (60:40% ratio) and cultured in DMEM/F12 medium supplemented with 20 ng/ml each of human EGF, human FGF, and 1X B27 in ultra-low attachment plates. Cells were then treated with either vehicle or GW296115 (2 μM) and GW296115 (3 μM) for another 72 h. Images were taken at 10X magnification using a Nikon Eclipse Ti-U Inverted Phase Contrast Microscope (Nikon Instruments Inc., USA). As described previously[109], the aggressive tumor cell invasion phenotypes were analyzed using ImageJ software (National Institute of Health, USA). The invasion of 3D spheroids was quantified as the average number of invadopodia/protrusions per spheroid (n = 5–10).

Cell growth assay

Cell growth assays were performed as described[109,119,120]. Briefly, cell growth was measured by adding WST-8 reagent (Dojindo Molecular Technologies, CK04) and incubating at 37 °C for 1 h. Absorbance was measured at 450 nm with background subtraction using a Microplate Reader (BioTek, USA).

Apoptotic cell death assay

Apoptotic cell death was measured by PARP cleavage, and activation of caspase-7 and caspase-9 were also determined with antibodies that recognize cleaved products as described previously[82,119].

Cytochrome c release from mitochondria into the cytosol was determined by immunoblotting with anti-cytochrome c as described previously[81,82].

Colony-forming assay

MDA-MB-231 cells (1×10^6 cells/well) were seeded on 6-well plates in a serum-containing medium the day before treatment. Vehicle or GW296115 (1 μM) was treated for two weeks. Following treatment, cells were washed with 1X PBS, fixed with 4% paraformaldehyde (Sigma-Aldrich, 158127) at RT for 10 min, and stained using crystal violet solution (0.05% crystal violet [Sigma-Aldrich, 61135], 1% formaldehyde [Sigma-Aldrich, F8775], 1% methanol [Fisher, A452-4] and 1X PBS) for 30 min at RT. Stained cells were washed with water and air-dried at room temperature. The number of colonies was counted using the inverted tissue culture microscope (Fisher Scientific, USA) with 4X magnification.

Cell migration assay

A wound healing/scratch assay was performed to test the migration ability of cells by measuring their motility. MDA-MB-231 cells were seeded in 6-well tissue culture plates at a 1.0 × 106 cells/well density and cultured in a growth medium for 24 h. Then, the cells were scratched by a sterile 200 μl pipette tip. Cellular debris was removed, and cells were gently washed with a fresh growth medium. The cells were treated with vehicle or GW296115 (2 μM) for 24 h. Wounded areas were photographed under an inverted microscope at time points 0 and 24 h after scratching.

Transmission electron microscopy

TEM analysis of the autophagosome was carried out as previously described[121]. The cells were exposed to an EBSS medium for 24 h and fixed with 2.5% glutaraldehyde in 0.1 M sodium cacodylate buffer. Samples are incubated on grids and negatively stained with 2% uranyl acetate, as described previously[109]. Imaging was performed on a Philips/FEI T-12 transmission electron microscope and analyzed by NIH ImageJ software.

Immunofluorescence imaging (GFP-LC3)

m-GFP tandem fluorescent-tagged LC3 (GFP-LC3) immunocytochemistry and fluorescence microscopy. MDA-MB-231 cells were transfected with GFP-LC3 plasmid (1 μg) vs. empty vector for 24 h. The next day, the cells were again transfected with the BRSK2 (0.75 μg) plasmid vs. the empty vector. For some experiments, cells were transfected with siBRSK2 or siControl for 24 h, and the next day, GFP-LC3 was transfected for an additional 24 h. After 24 h of the second transfection, cells were transferred to control media and nutrient-deprived media (EBSS) for an additional 6 h. After treatment, cells were washed and fixed with 4% paraformaldehyde and then mounted onto microscope slides. Localization of GFP-LC3 was examined with a Nikon inverted fluorescence microscope. For some experiments, ZOE Fluorescent Cell Imager (Bio-Rad) and EVOS FL (Life Technologies) were used for GFP-LC3 imaging. All the images were acquired with fixed exposure time and parameters. Images were processed using Fiji/ImageJ software (National Institutes of Health, USA). Four fields of view from two biological replicates were assessed[122]. GFP-LC3 puncta staining was counted from at least n = 20 cells/sample, with GFP-positive cells selected randomly from fields for scoring per condition to quantify autophagy.

Breast cancer cohort data analysis

Breast cancer cohort data from patients were analyzed as described previously[75,109,115]. Publicly available clinical parameters and tumor gene expression data were acquired from The Cancer Genome Atlas (TCGA) breast cancer cohort[41] and the Molecular Taxonomy of Breast Cancer International Consortium (METABRIC) cohort[42] for analysis through cBioportal[123]. Regarding survival data, disease-specific survival (DSS) and other forms of patient survival were available in TCGA breast cancer cohort and the METABRIC cohort. Univariate

Cox regression analysis was performed using the cohorts to determine which gene's expression may be an independent prognostic marker for patient survival. Any gene's high/low cutoff was defined as the top third vs. the bottom two-thirds within any cohort.

Source of breast cancer human tissues for BRSK2 gene expression analysis

We have obtained de-identified human primary breast tumor tissue clinical specimens from the Data Bank and BioRepository Shared Resources (BDDR) at RPCCC, with Institutional Review Board approval (RPCCC, BDR #074516). The detailed clinical characteristics (hormone receptor status, age, stage, and history of distant metastasis) of breast cancer patients were described previously[44].

Statistical analysis

Quantitative data are presented as mean ± standard error (s.e.) of three independent replicates. We have used a one-way ANOVA test for datasets containing multiple group comparisons and Tukey's post hoc test for the family-wise error rate comparison. Association between variables (e.g., gene expression scores) was determined using the Mann–Whitney U test. Kaplan–Meier method with the log-rank test was used to compare survival curves between groups. All statistical tests were performed using the GraphPad Prism 8 software. $p < 0.05$ was considered statistically significant.

Data availability

The datasets analyzed during the current study are available in The Cancer Genome Atlas repository, [https://portal.gdc.cancer.gov/projects/TCGA-BRCA], and the METABRIC repository. [https://www.cbioportal.org/study/summary?id=brca_metabric]. The data that support the findings of this study are available from the corresponding authors upon reasonable request.

Received: 25 March 2025; Accepted: 13 October 2025
Published online: 19 November 2025

References

1. Steeg, P. S. Targeting metastasis. *Nat. Rev. Cancer* **16**, 201–218. https://doi.org/10.1038/nrc.2016.25 (2016).
2. Mowers, E. E., Sharifi, M. N. & Macleod, K. F. Autophagy in cancer metastasis. *Oncogene* **36**, 1619–1630. https://doi.org/10.1038/onc.2016.333 (2017).
3. Kenific, C. M., Thorburn, A. & Debnath, J. Autophagy and metastasis: Another double-edged sword. *Curr. Opin. Cell Biol.* **22**, 241–245. https://doi.org/10.1016/j.ceb.2009.10.008 (2010).
4. Gundamaraju, R. et al. Autophagy and EMT in cancer and metastasis: Who controls whom?. *Biochim. Biophys. Acta Mol. Basis Dis.* **1868**, 166431. https://doi.org/10.1016/j.bbadis.2022.166431 (2022).
5. Alizadeh, J., Lorzadeh, S. & Ghavami, S. Autophagy and cancer metastasis: A trojan horse. *J. Investig. Med.* **69**, 1145–1147. https://doi.org/10.1136/jim-2021-002016 (2021).
6. Chen, H. T. et al. Crosstalk between autophagy and epithelial-mesenchymal transition and its application in cancer therapy. *Mol. Cancer* **18**, 101. https://doi.org/10.1186/s12943-019-1030-2 (2019).
7. Duan, Z. et al. Autophagy-associated immunogenic modulation and its applications in cancer therapy. *Cells* **11**, 2324. https://doi.org/10.3390/cells11152324 (2022).
8. Degenhardt, K. et al. Autophagy promotes tumor cell survival and restricts necrosis, inflammation, and tumorigenesis. *Cancer Cell* **10**, 51–64. https://doi.org/10.1016/j.ccr.2006.06.001 (2006).
9. Avivar-Valderas, A. et al. Regulation of autophagy during ECM detachment is linked to a selective inhibition of mTORC1 by PERK. *Oncogene* **32**, 4932–4940. https://doi.org/10.1038/onc.2012.512 (2013).
10. Fung, C., Lock, R., Gao, S., Salas, E. & Debnath, J. Induction of autophagy during extracellular matrix detachment promotes cell survival. *Mol. Biol. Cell* **19**, 797–806. https://doi.org/10.1091/mbc.e07-10-1092 (2008).
11. Vera-Ramirez, L., Vodnala, S. K., Nini, R., Hunter, K. W. & Green, J. E. Autophagy promotes the survival of dormant breast cancer cells and metastatic tumour recurrence. *Nat. Commun.* **9**, 1944. https://doi.org/10.1038/s41467-018-04070-6 (2018).
12. Lazova, R. et al. Punctate LC3B expression is a common feature of solid tumors and associated with proliferation, metastasis, and poor outcome. *Clin. Cancer Res.* **18**, 370–379. https://doi.org/10.1158/1078-0432.CCR-11-1282 (2012).
13. Qiang, L. & He, Y. Y. Autophagy deficiency stabilizes TWIST1 to promote epithelial-mesenchymal transition. *Autophagy* **10**, 1864–1865. https://doi.org/10.4161/auto.32171 (2014).
14. Bertrand, M. et al. SQSTM1/p62 regulates the expression of junctional proteins through epithelial-mesenchymal transition factors. *Cell Cycle* **14**, 364–374. https://doi.org/10.4161/15384101.2014.987619 (2015).
15. Mohsen, S. et al. Autophagy agents in clinical trials for cancer therapy: A brief review. *Curr. Oncol.* **29**, 1695–1708. https://doi.org/10.3390/curroncol29030141 (2022).
16. Wolpin, B. M. et al. Phase II and pharmacodynamic study of autophagy inhibition using hydroxychloroquine in patients with metastatic pancreatic adenocarcinoma. *Oncologist* **19**, 637–638. https://doi.org/10.1634/theoncologist.2014-0086 (2014).
17. Yang, Z. & Klionsky, D. J. Eaten alive: A history of macroautophagy. *Nat. Cell Biol.* **12**, 814–822. https://doi.org/10.1038/ncb0910-814 (2010).
18. Mizushima, N., Levine, B., Cuervo, A. M. & Klionsky, D. J. Autophagy fights disease through cellular self-digestion. *Nature* **451**, 1069–1075. https://doi.org/10.1038/nature06639 (2008).
19. Levine, B. & Klionsky, D. J. Development by self-digestion: Molecular mechanisms and biological functions of autophagy. *Dev. Cell* **6**, 463–477. https://doi.org/10.1016/s1534-5807(04)00099-1 (2004).
20. Anderson, C. M. & Macleod, K. F. Autophagy and cancer cell metabolism. *Int. Rev. Cell Mol. Biol.* **347**, 145–190. https://doi.org/10.1016/bs.ircmb.2019.06.002 (2019).
21. Meijer, A. J., Lorin, S., Blommaart, E. F. & Codogno, P. Regulation of autophagy by amino acids and MTOR-dependent signal transduction. *Amino Acids* **47**, 2037–2063. https://doi.org/10.1007/s00726-014-1765-4 (2015).
22. Russell, R. C. et al. ULK1 induces autophagy by phosphorylating Beclin-1 and activating VPS34 lipid kinase. *Nat. Cell Biol.* **15**, 741–750. https://doi.org/10.1038/ncb2757 (2013).
23. Ktistakis, N. T. & Tooze, S. A. Digesting the expanding mechanisms of autophagy. *Trends Cell Biol.* **26**, 624–635. https://doi.org/10.1016/j.tcb.2016.03.006 (2016).
24. Mihaylova, M. M. & Shaw, R. J. The AMPK signalling pathway coordinates cell growth, autophagy and metabolism. *Nat. Cell Biol.* **13**, 1016–1023. https://doi.org/10.1038/ncb2329 (2011).

25. Bright, N. J., Carling, D. & Thornton, C. Investigating the regulation of brain-specific kinases 1 and 2 by phosphorylation. *J. Biol. Chem.* **283**, 14946–14954. https://doi.org/10.1074/jbc.M710381200 (2008).
26. Lizcano, J. M. et al. LKB1 is a master kinase that activates 13 kinases of the AMPK subfamily, including MARK/PAR-1. *EMBO J.* **23**, 833–843. https://doi.org/10.1038/sj.emboj.7600110 (2004).
27. Nie, J. et al. Synapses of amphids defective (SAD-A) kinase promotes glucose-stimulated insulin secretion through activation of p21-activated kinase (PAK1) in pancreatic beta-cells. *J. Biol. Chem.* **287**, 26435–26444. https://doi.org/10.1074/jbc.M112.378372 (2012).
28. Consortium GT. The Genotype-Tissue Expression (GTEx) project. *Nat. Genet.* **45**, 580–585. https://doi.org/10.1038/ng.2653 (2013).
29. Kishi, M., Pan, Y. A., Crump, J. G. & Sanes, J. R. Mammalian SAD kinases are required for neuronal polarization. *Science* **307**, 929–932. https://doi.org/10.1126/science.1107403 (2005).
30. Dhumale, P., Menon, S., Chiang, J. & Puschel, A. W. The loss of the kinases SadA and SadB results in early neuronal apoptosis and a reduced number of progenitors. *PLoS ONE* **13**, e0196698. https://doi.org/10.1371/journal.pone.0196698 (2018).
31. Chen, X. Y. et al. Brain-selective kinase 2 (BRSK2) phosphorylation on PCTAIRE1 negatively regulates glucose-stimulated insulin secretion in pancreatic beta-cells. *J. Biol. Chem.* **287**, 30368–30375. https://doi.org/10.1074/jbc.M112.375618 (2012).
32. Nie, J., Sun, C., Chang, Z., Musi, N. & Shi, Y. SAD-A promotes glucose-stimulated insulin secretion through phosphorylation and inhibition of GDIalpha in male islet beta cells. *Endocrinology* **159**, 3036–3047. https://doi.org/10.1210/en.2017-03243 (2018).
33. Bakula, D. et al. WIPI3 and WIPI4 beta-propellers are scaffolds for LKB1-AMPK-TSC signalling circuits in the control of autophagy. *Nat. Commun.* **8**, 15637. https://doi.org/10.1038/ncomms15637 (2017).
34. Saiyin, H. et al. BRSK2 induced by nutrient deprivation promotes Akt activity in pancreatic cancer via downregulation of mTOR activity. *Oncotarget* **8**, 44669–44681. https://doi.org/10.18632/oncotarget.17965 (2017).
35. Tamir, T. Y., Drewry, D. H., Wells, C., Major, M. B. & Axtman, A. D. PKIS deep dive yields a chemical starting point for dark kinases and a cell active BRSK2 inhibitor. *Sci. Rep.* **10**, 15826. https://doi.org/10.1038/s41598-020-72869-9 (2020).
36. Tamir, T. Y. et al. Gain-of-function genetic screen of the kinome reveals BRSK2 as an inhibitor of the NRF2 transcription factor. *J. Cell Sci.* **133**, jcs241356. https://doi.org/10.1242/jcs.241356 (2020).
37. Wang, Y., Wan, B., Zhou, J., Li, R. & Yu, L. BRSK2 is a valosin-containing protein (VCP)-interacting protein that affects VCP functioning in endoplasmic reticulum-associated degradation. *Biotechnol. Lett.* **35**, 1983–1989. https://doi.org/10.1007/s10529-013-1295-2 (2013).
38. Wang, Y. et al. BRSK2 is regulated by ER stress in protein level and involved in ER stress-induced apoptosis. *Biochem. Biophys. Res. Commun.* **423**, 813–818. https://doi.org/10.1016/j.bbrc.2012.06.046 (2012).
39. Bhaskar, P. T. & Hay, N. The two TORCs and Akt. *Dev. Cell* **12**, 487–502. https://doi.org/10.1016/j.devcel.2007.03.020 (2007).
40. Manning, B. D. et al. Feedback inhibition of Akt signaling limits the growth of tumors lacking Tsc2. *Genes Dev.* **19**, 1773–1778. https://doi.org/10.1101/gad.1314605 (2005).
41. Cancer Genome Atlas, N. Comprehensive molecular portraits of human breast tumours. *Nature* **490**, 61–70. https://doi.org/10.1038/nature11412 (2012).
42. Curtis, C. et al. The genomic and transcriptomic architecture of 2000 breast tumours reveals novel subgroups. *Nature* **486**, 346–352. https://doi.org/10.1038/nature10983 (2012).
43. Niu, G. M., Ji, Y., Jin, D. Y., Hou, J. & Lou, W. H. Clinical implication of BRSK2 expression in pancreatic ductal adenocarcinoma. *Zhonghua Yi Xue Za Zhi* **90**, 1084–1088 (2010).
44. McDonald, K. A. et al. Development of KAM score to predict metastasis and worse survival in breast cancer. *Am. J. Cancer Res.* **11**, 5388–5401 (2021).
45. Wang, H. et al. Decreased expression and prognostic role of cytoplasmic BRSK1 in human breast carcinoma: Correlation with Jab1 stability and PI3K/Akt pathway. *Exp. Mol. Pathol.* **97**, 191–201. https://doi.org/10.1016/j.yexmp.2014.07.012 (2014).
46. Choi, E. J., Yoo, N. J., Kim, M. S., An, C. H. & Lee, S. H. Putative tumor suppressor genes EGR1 and BRSK1 are mutated in gastric and colorectal cancers. *Oncology* **91**, 289–294. https://doi.org/10.1159/000450616 (2016).
47. Zhou, J. et al. Jab1 interacts with brain-specific kinase 2 (BRSK2) and promotes its degradation in the ubiquitin-proteasome pathway. *Biochem. Biophys. Res. Commun.* **422**, 647–652. https://doi.org/10.1016/j.bbrc.2012.05.045 (2012).
48. Li, R. et al. APC/C(Cdh1) targets brain-specific kinase 2 (BRSK2) for degradation via the ubiquitin-proteasome pathway. *PLoS ONE* **7**, e45932. https://doi.org/10.1371/journal.pone.0045932 (2012).
49. Su, Y., Pogash, T. J., Nguyen, T. D. & Russo, J. Development and characterization of two human triple-negative breast cancer cell lines with highly tumorigenic and metastatic capabilities. *Cancer Med.* **5**, 558–573. https://doi.org/10.1002/cam4.616 (2016).
50. McKenna, M., McGarrigle, S. & Pidgeon, G. P. The next generation of PI3K-Akt-mTOR pathway inhibitors in breast cancer cohorts. *Biochim. Biophys. Acta Rev. Cancer* **1185–197**, 2018. https://doi.org/10.1016/j.bbcan.2018.08.001 (1870).
51. Devarajan, E. & Huang, S. STAT3 as a central regulator of tumor metastases. *Curr. Mol. Med.* **9**, 626–633 (2009).
52. Xia, Y., Shen, S. & Verma, I. M. NF-kappaB, an active player in human cancers. *Cancer Immunol. Res.* **2**, 823–830. https://doi.org/10.1158/2326-6066.CIR-14-0112 (2014).
53. Ji, Z., He, L., Regev, A. & Struhl, K. Inflammatory regulatory network mediated by the joint action of NF-kB, STAT3, and AP-1 factors is involved in many human cancers. *Proc. Natl. Acad. Sci. USA* **116**, 9453–9462. https://doi.org/10.1073/pnas.1821068116 (2019).
54. Yang, J. et al. Targeting PI3K in cancer: Mechanisms and advances in clinical trials. *Mol. Cancer* **18**, 26. https://doi.org/10.1186/s12943-019-0954-x (2019).
55. Yang, L., Han, S. & Sun, Y. An IL6-STAT3 loop mediates resistance to PI3K inhibitors by inducing epithelial-mesenchymal transition and cancer stem cell expansion in human breast cancer cells. *Biochem. Biophys. Res. Commun.* **453**, 582–587. https://doi.org/10.1016/j.bbrc.2014.09.129 (2014).
56. Vasudevan, K. M., Gurumurthy, S. & Rangnekar, V. M. Suppression of PTEN expression by NF-kappa B prevents apoptosis. *Mol. Cell. Biol.* **24**, 1007–1021. https://doi.org/10.1128/MCB.24.3.1007-1021.2004 (2004).
57. Ishiguro, T. et al. Tumor-derived spheroids: Relevance to cancer stem cells and clinical applications. *Cancer Sci.* **108**, 283–289. https://doi.org/10.1111/cas.13155 (2017).
58. Khaitan, D., Chandna, S., Arya, M. B. & Dwarakanath, B. S. Establishment and characterization of multicellular spheroids from a human glioma cell line; Implications for tumor therapy. *J. Transl. Med.* **4**, 12–5876–5874–5812, 1479–5876–4–12 [pii] (2006).
59. Wainwright, E. N. & Scaffidi, P. Epigenetics and cancer stem cells: Unleashing, hijacking, and restricting cellular plasticity. *Trends Cancer* **3**, 372–386 (2017) (**S2405-8033(17)30081-X [pii]**).
60. Grivennikov, S. I. & Karin, M. Dangerous liaisons: STAT3 and NF-kappaB collaboration and crosstalk in cancer. *Cytokine Growth Factor Rev.* **21**, 11–19. https://doi.org/10.1016/j.cytogfr.2009.11.005 (2010).
61. Carpenter, R. L. & Lo, H. W. STAT3 Target Genes Relevant to Human Cancers. *Cancers* **6**, 897–925. https://doi.org/10.3390/cancers6020897 (2014).
62. Zhang, T., Ma, C., Zhang, Z., Zhang, H. & Hu, H. NF-kappaB signaling in inflammation and cancer. *MedComm* **2020**(2), 618–653. https://doi.org/10.1002/mco2.104 (2021).
63. Osawa, T. & Shibuya, M. Targeting cancer cells resistant to hypoxia and nutrient starvation to improve anti-angiogeneic therapy. *Cell Cycle* **12**, 2519–2520. https://doi.org/10.4161/cc.25729 (2013).
64. Osawa, T. et al. Inhibition of histone demethylase JMJD1A improves anti-angiogenic therapy and reduces tumor-associated macrophages. *Cancer Res.* **73**, 3019–3028. https://doi.org/10.1158/0008-5472.CAN-12-3231 (2013).

65. Muniraj, N. et al. Induction of STK11-dependent cytoprotective autophagy in breast cancer cells upon honokiol treatment. *Cell Death Discov.* **6**, 81. https://doi.org/10.1038/s41420-020-00315-w (2020).
66. Lefort, S. et al. Inhibition of autophagy as a new means of improving chemotherapy efficiency in high-LC3B triple-negative breast cancers. *Autophagy* **10**, 2122–2142. https://doi.org/10.4161/15548627.2014.981788 (2014).
67. Vijayaraghavan, S. et al. CDK4/6 and autophagy inhibitors synergistically induce senescence in Rb positive cytoplasmic cyclin E negative cancers. *Nat. Commun.* **8**, 15916. https://doi.org/10.1038/ncomms15916 (2017).
68. Lin, J. Y. & Huang, H. I. Autophagy is induced and supports virus replication in Enterovirus A71-infected human primary neuronal cells. *Sci. Rep.* **10**, 15234. https://doi.org/10.1038/s41598-020-71970-3 (2020).
69. Liebl, M. P. et al. Robust LC3B lipidation analysis by precisely adjusting autophagic flux. *Sci. Rep.* **12**, 79. https://doi.org/10.1038/s41598-021-03875-8 (2022).
70. Huang, S. S. et al. Resveratrol protects podocytes against apoptosis via stimulation of autophagy in a mouse model of diabetic nephropathy. *Sci. Rep.* **7**, 45692. https://doi.org/10.1038/srep45692 (2017).
71. Ivanova, O. A. et al. LMNA R482L mutation causes impairments in C2C12 myoblasts subpopulations, alterations in metabolic reprogramming during differentiation, and oxidative stress. *Sci. Rep.* **15**, 5358. https://doi.org/10.1038/s41598-025-88219-6 (2025).
72. Loos, B., du Toit, A. & Hofmeyr, J. H. Defining and measuring autophagosome flux-concept and reality. *Autophagy* **10**, 2087–2096. https://doi.org/10.4161/15548627.2014.973338 (2014).
73. Chu, H. Y. et al. Bafilomycin A1 increases the sensitivity of tongue squamous cell carcinoma cells to cisplatin by inhibiting the lysosomal uptake of platinum ions but not autophagy. *Cancer Lett.* **423**, 105–112. https://doi.org/10.1016/j.canlet.2018.03.003 (2018).
74. Peeters, J. G. C. et al. Transcriptional and epigenetic profiling of nutrient-deprived cells to identify novel regulators of autophagy. *Autophagy* **15**, 98–112. https://doi.org/10.1080/15548627.2018.1509608 (2019).
75. Hait, N. C. et al. Regulation of hypoxia-inducible factor functions in the nucleus by sphingosine-1-phosphate. *FASEB J.* **34**, 4293–4310. https://doi.org/10.1096/fj.201901734RR (2020).
76. Giuliani, C. et al. Epigenetic variability across human populations: A focus on DNA methylation profiles of the KRTCAP3, MAD1L1 and BRSK2 genes. *Genome Biol. Evol.* **8**, 2760–2773. https://doi.org/10.1093/gbe/evw186 (2016).
77. Kim, I. & Park, J. W. Hypoxia-driven epigenetic regulation in cancer progression: A focus on histone methylation and its modifying enzymes. *Cancer Lett.* **489**, 41–49. https://doi.org/10.1016/j.canlet.2020.05.025 (2020).
78. Marino, G., Niso-Santano, M., Baehrecke, E. H. & Kroemer, G. Self-consumption: The interplay of autophagy and apoptosis. *Nat. Rev. Mol. Cell Biol.* **15**, 81–94. https://doi.org/10.1038/nrm3735 (2014).
79. Gong, C. *et al.* Beclin 1 and autophagy are required for the tumorigenicity of breast cancer stem-like/progenitor cells. *Oncogene* **32**, 2261–2272, 2272e 2261–2211, (2013) https://doi.org/10.1038/onc.2012.252.
80. Bjorkoy, G. et al. Monitoring autophagic degradation of p62/SQSTM1. *Methods Enzymol.* **452**, 181–197. https://doi.org/10.1016/S0076-6879(08)03612-4 (2009).
81. Maceyka, M. et al. SphK1 and SphK2, sphingosine kinase isoenzymes with opposing functions in sphingolipid metabolism. *J. Biol. Chem.* **280**, 37118–37129 (2005) (**M502207200[pii]**).
82. Sankala, H. M. et al. Involvement of sphingosine kinase 2 in p53-independent induction of p21 by the chemotherapeutic drug doxorubicin. *Cancer Res.* **67**, 10466–10474 (2007) (**67/21/10466[pii]**).
83. Cho, K. J., Shin, S. Y., Moon, H., Kim, B. K. & Ro, S. W. Knockdown of Atg7 suppresses Tumorigenesis in a murine model of liver cancer. *Transl. Oncol.* **14**, 101158. https://doi.org/10.1016/j.tranon.2021.101158 (2021).
84. Maheshwari, M. et al. Inhibition of p21 activates Akt kinase to trigger ROS-induced autophagy and impacts on tumor growth rate. *Cell Death Dis.* **13**, 1045. https://doi.org/10.1038/s41419-022-05486-1 (2022).
85. Xu, D. Q. et al. PAQR3 controls autophagy by integrating AMPK signaling to enhance ATG14L-associated PI3K activity. *EMBO J.* **35**, 496–514. https://doi.org/10.15252/embj.201592864 (2016).
86. He, L. et al. Autophagy: The last defense against cellular nutritional stress. *Adv. Nutr.* **9**, 493–504. https://doi.org/10.1093/advances/nmy011 (2018).
87. Kroemer, G., Marino, G. & Levine, B. Autophagy and the integrated stress response. *Mol. Cell* **40**, 280–293. https://doi.org/10.1016/j.molcel.2010.09.023 (2010).
88. Bertout, J. A., Patel, S. A. & Simon, M. C. The impact of O_2 availability on human cancer. *Nat. Rev. Cancer* **8**, 967–975. https://doi.org/10.1038/nrc2540 (2008).
89. Kim, J. & DeBerardinis, R. J. Mechanisms and implications of metabolic heterogeneity in cancer. *Cell Metab.* **30**, 434–446. https://doi.org/10.1016/j.cmet.2019.08.013 (2019).
90. Debnath, J. The multifaceted roles of autophagy in tumors-implications for breast cancer. *J. Mammary Gland Biol. Neoplasia* **16**, 173–187. https://doi.org/10.1007/s10911-011-9223-3 (2011).
91. Sabater, L., Gomez-Choco, M., Saiz, A. & Graus, F. BR serine/threonine kinase 2: A new autoantigen in paraneoplastic limbic encephalitis. *J. Neuroimmunol.* **170**, 186–190. https://doi.org/10.1016/j.jneuroim.2005.08.011 (2005).
92. Chen, Z., Han, F., Du, Y., Shi, H. & Zhou, W. Hypoxic microenvironment in cancer: Molecular mechanisms and therapeutic interventions. *Signal Transduct. Target. Ther.* **8**, 70. https://doi.org/10.1038/s41392-023-01332-8 (2023).
93. Southekal, S., Mishra, N. K. & Guda, C. Pan-cancer analysis of human kinome gene expression and promoter DNA methylation identifies dark kinase biomarkers in multiple cancers. *Cancers* **13**, 1189. https://doi.org/10.3390/cancers13061189 (2021).
94. Gritsko, T. et al. Persistent activation of stat3 signaling induces survivin gene expression and confers resistance to apoptosis in human breast cancer cells. *Clin. Cancer Res. Off. J. Am. Assoc. Cancer Res.* **12**, 11–19 (2006) (**12/1/11[pii]**).
95. Oeckinghaus, A. & Ghosh, S. The NF-kappaB family of transcription factors and its regulation. *Cold Spring. Harb. Perspect. Biol.* **1**, a000034. https://doi.org/10.1101/cshperspect.a000034 (2009).
96. Zinatizadeh, M. R. et al. The nuclear factor kappa B (NF-kB) signaling in cancer development and immune diseases. *Genes Dis.* **8**, 287–297. https://doi.org/10.1016/j.gendis.2020.06.005 (2021).
97. Khongthong, P., Roseweir, A. K. & Edwards, J. The NF-KB pathway and endocrine therapy resistance in breast cancer. *Endocr. Relat. Cancer* **26**, R369–R380. https://doi.org/10.1530/ERC-19-0087 (2019).
98. Dolcet, X., Llobet, D., Pallares, J. & Matias-Guiu, X. NF-kB in development and progression of human cancer. *Virchows Arch.* **446**, 475–482. https://doi.org/10.1007/s00428-005-1264-9 (2005).
99. Yoon, S. et al. STAT3 transcriptional factor activated by reactive oxygen species induces IL6 in starvation-induced autophagy of cancer cells. *Autophagy* **6**, 1125–1138. https://doi.org/10.4161/auto.6.8.13547 (2010).
100. Soria, G. et al. Inflammatory mediators in breast cancer: coordinated expression of TNFalpha & IL-1beta with CCL2 & CCL5 and effects on epithelial-to-mesenchymal transition. *BMC Cancer* **11**, 130. https://doi.org/10.1186/1471-2407-11-130 (2011).
101. Richmond, A. Nf-kappa B, chemokine gene transcription and tumour growth. *Nat. Rev. Immunol.* **2**, 664–674. https://doi.org/10.1038/nri887 (2002).
102. Karantza-Wadsworth, V. et al. Autophagy mitigates metabolic stress and genome damage in mammary tumorigenesis. *Genes Dev.* **21**, 1621–1635. https://doi.org/10.1101/gad.1565707 (2007).
103. Monkkonen, T. & Debnath, J. Inflammatory signaling cascades and autophagy in cancer. *Autophagy* **14**, 190–198. https://doi.org/10.1080/15548627.2017.1345412 (2018).
104. Maiti, A. & Hait, N. C. Autophagy-mediated tumor cell survival and progression of breast cancer metastasis to the brain. *J. Cancer* **12**, 954–964. https://doi.org/10.7150/jca.50137 (2021).

105. Kaverina, N. et al. Astrocytes promote progression of breast cancer metastases to the brain via a KISS1-mediated autophagy. *Autophagy* **13**, 1905–1923. https://doi.org/10.1080/15548627.2017.1360466 (2017).
106. Trocoli, A. & Djavaheri-Mergny, M. The complex interplay between autophagy and NF-kappaB signaling pathways in cancer cells. *Am. J. Cancer Res.* **1**, 629–649 (2011).
107. Kma, L. & Baruah, T. J. The interplay of ROS and the PI3K/Akt pathway in autophagy regulation. *Biotechnol. Appl. Biochem.* **69**, 248–264. https://doi.org/10.1002/bab.2104 (2022).
108. Maiti, A., Takabe, K. & Hait, N. C. Metastatic triple-negative breast cancer is dependent on SphKs/S1P signaling for growth and survival. *Cell. Signal.* **32**, 85–92 (2017) (**S0898-6568(17)30025-6[pii]**).
109. Hait, N. C. et al. Extracellular sialyltransferase st6gal1 in breast tumor cell growth and invasiveness. *Cancer Gene Ther.* https://doi.org/10.1038/s41417-022-00485-y (2022).
110. Maiti, A. et al. Class I histone deacetylase inhibitor suppresses vasculogenic mimicry by enhancing the expression of tumor suppressor and anti-angiogenesis genes in aggressive human TNBC cells. *Int. J. Oncol.* https://doi.org/10.3892/ijo.2019.4796 (2019).
111. Hait, N. C., Bellamy, A., Milstien, S., Kordula, T. & Spiegel, S. Sphingosine kinase type 2 activation by ERK-mediated phosphorylation. *J. Biol. Chem.* **282**, 12058–12065 (2007) (**M609559200[pii]**).
112. Opyrchal, M. et al. Inhibition of Cdk2 kinase activity selectively targets the CD44(+)/CD24(-)/Low stem-like subpopulation and restores chemosensitivity of SUM149PT triple-negative breast cancer cells. *Int. J. Oncol.* **45**, 1193–1199. https://doi.org/10.3892/ijo.2014.2523 (2014).
113. Gril, B. et al. Reactive astrocytic S1P3 signaling modulates the blood-tumor barrier in brain metastases. *Nat. Commun.* **9**, 2705. https://doi.org/10.1038/s41467-018-05030-w (2018).
114. Hait, N. C. et al. Regulation of histone acetylation in the nucleus by sphingosine-1-phosphate. *Sci. N. Y.* **325**, 1254–1257. https://doi.org/10.1126/science.1176709 (2009).
115. Maiti, A. et al. Altered Expression of Secreted Mediator Genes That Mediate Aggressive Breast Cancer Metastasis to Distant Organs. *Cancers* **13**, 2641. https://doi.org/10.3390/cancers13112641 (2021).
116. Hait, N. C. et al. Active, phosphorylated fingolimod inhibits histone deacetylases and facilitates fear extinction memory. *Nat. Neurosci.* **17**, 971–980. https://doi.org/10.1038/nn.3728 (2014).
117. Luca, R. et al. The fragile X protein binds mRNAs involved in cancer progression and modulates metastasis formation. *EMBO Mol. Med.* **5**, 1523–1536. https://doi.org/10.1002/emmm.201302847 (2013).
118. Berens, E. B., Holy, J. M., Riegel, A. T. & Wellstein, A. A cancer cell spheroid assay to assess invasion in a 3D setting. *J. Vis. Exp.* https://doi.org/10.3791/53409 (2015).
119. Sarkar, S. et al. Sphingosine kinase 1 is required for migration, proliferation and survival of MCF-7 human breast cancer cells. *FEBS Lett.* **579**, 5313–5317 (2005) (**S0014-5793(05)01067-7[pii]**).
120. Hait, N. C. et al. Role of sphingosine kinase 2 in cell migration toward epidermal growth factor. *J. Biol. Chem.* **280**, 29462–29469 (2005) (**M502922200[pii]**).
121. Zhang, Q. et al. Transfer of Functional Cargo in Exomeres. *Cell Rep.* **27**, 940–954. https://doi.org/10.1016/j.celrep.2019.01.009 (2019).
122. Schindelin, J. et al. Fiji: An open-source platform for biological-image analysis. *Nat. Methods* **9**, 676–682. https://doi.org/10.1038/nmeth.2019 (2012).
123. Cerami, E. et al. The cBio cancer genomics portal: An open platform for exploring multidimensional cancer genomics data. *Cancer Discov.* **2**, 401–404. https://doi.org/10.1158/2159-8290.CD-12-0095 (2012).

Acknowledgments

This work was supported by grants 1R03CA280307 and Roswell Park Health Research Incorporated (HRI) Start-Up Funds #714084-01 and Department of Defense (DoD) Award number: HT94252410762 to NCH and R01CA250412 to SSE. The core facilities of RPCCC used in this work were supported in part by NIH National Cancer Institute Cancer Center Support Grant P30CA16056. We thank Dr. Santosh Patnaik (Thoracic Surgery, RPCCC) for the additional help with bioinformatics. We also thank Mr. Donald MacFarland, Lead Electron Microscopist at the University at Buffalo, Jacobs School of Medicine, Buffalo, NY, USA, for the TEM analysis.

Author contributions

Study concept and design: N.C.H. and A.M. Acquisition of data: N.C.H., A.M., L.Y., A.B.S. Analysis and interpretation of data: N.C.H., A.M., A.D.A., L.J.B.R., K.T., A.B.S., L.Y., M.J.C., J.Z., S.S.E., and P.K. Bioinformatics: L.Y. and R.W. Material support: A.D.A. Study supervision: N.C.H. and A.M. Manuscript writing: N.C.H. and A.M. Manuscript review and editing: N.C.H., A.M., A.D.A., L.J.B.R., K.T., A.B.S., L.Y., M.J.C., J.Z., S.S.E., and P.K.

Declarations

Competing interests

The authors declare no competing interests.

Additional information

Supplementary Information The online version contains supplementary material available at https://doi.org/10.1038/s41598-025-24354-4.

Correspondence and requests for materials should be addressed to A.M. or N.C.H.